# Chemical Exploits with Actinide Ions in the Gas Phase: Insights into Actinyl Hydration, 5f Bonding, and More

J. K. Gibson*, R. G. Haire*, M. Santos†, J. Marçalo†, A. Pires de Matos†

*Chemical Sciences Division, Oak Ridge National Laboratory, Oak Ridge TN 37831, USA
† Departamento de Química, Instituto Tecnológico e Nuclear, 2686-953 Sacavém, Portugal

## INTRODUCTION

Systematic studies of gas-phase reactions involving bare and ligated monopositive and dipositive actinide ions are contributing to fundamental aspects of actinide science. Using Fourier transform ion cyclotron resonance mass spectrometry, we can manipulate actinide ions and perform complex reaction sequences. Such experiments reveal products and kinetics for reactions of actinide-containing ions with neutral reagents under bimolecular reaction conditions. Among the information that can be deduced are thermodynamic properties of actinide molecules and the role of the 5f electrons in molecular actinide chemistry. Oxidation reactions, actinide oxide thermodynamics, and reactivities of actinide oxide ions will be discussed.

## RESULTS AND DISCUSSION

The bare dipositive actinyl ions, $UO_2^{2+}$, $NpO_2^{2+}$, and $PuO_2^{2+}$, were produced from the reaction given by Eqn. (1) for An = U,[1,2] Np,[2] and Pu.[2]

$$AnO^{2+} + N_2O \rightarrow AnO_2^{2+} + N_2 \qquad (1)$$

The IE[$AnO_2^{+}$] were obtained from the measured relative rates of electron-transfer from selected neutral molecules to the three $AnO_2^{2+}$.[2] These ionization energies, together with known thermodynamic quantities, provide the formation enthalpies, $\Delta H_f[AnO_2^{2+}]$. After adjusting for the different standard states for the gas-phase and aqueous actinyls, the differences between our $\Delta H_f[AnO_2^{2+}]$ for the bare gas-phase ions and the known $\Delta H_f[AnO_2^{2+}(aq)]$ provide experimental values for the actinyl hydration enthalpies: $\Delta H_{hyd}[AnO_2^{2+}] \sim \Delta H_f[AnO_2^{2+}(aq)] - \Delta H_f[AnO_2^{2+}]$. The three values,[2] $\Delta H_{hyd}[UO_2^{2+}] = -1665\pm64$ kJ mol$^{-1}$, $\Delta H_{hyd}[NpO_2^{2+}] = -1654\pm91$ kJ mol$^{-1}$, and $\Delta H_{hyd}[PuO_2^{2+}] = -1671\pm67$ kJ mol$^{-1}$, are the same within the assigned uncertainties. Our experimental value for $\Delta H_{hyd}[UO_2^{2+}]$ is in remarkably good agreement with the value of -1676 kJ mol$^{-1}$ from DFT calculations.[3] From a subsequent DFT study[4] the derived $\Delta H_{hyd}[AnO_2^{2+}]$ are in the narrow range of -1615 to -1632 kJ mol$^{-1}$ for An = U, Np, and Pu, which are in reasonable agreement with our experimental values and our conclusion that the three actinyl hydration enthalpies are very similar to one another.

In a recent study,[5] we prepared the bare dipositive "protactinyl" ion, $PaO_2^{2+}$, via Eqn. (1) (An = Pa). In contrast to the three other actinyls discussed above, protactinyl is not stable in the condensed phase. It is now possible to estimate formation enthalpies for five actinyls, including americyl, which provide enthalpies for the atomization reaction in Eqn. (2).

$$AnO_2^{2+} \rightarrow An^{2+} + 2O \qquad (2)$$

The approximate atomization enthalpies are as follows (in kJ mol$^{-1}$), listed in order of decreasing actinyl stability:

**$UO_2^{2+}$ / 1250 > $PaO_2^{2+}$ / 1110 > $NpO_2^{2+}$ / 1030 > $PuO_2^{2+}$ / 830 > $AmO_2^{2+}$ / 600**

The decrease in stability between $UO_2^{2+}$ and $AmO_2^{2+}$ is in accord with aqueous chemistry. The high intrinsic stability of $PaO_2^{2+}$ is remarkable and is attributed to the very strong $Pa^{2+}$-O bond: $D[Pa^{2+}\text{-}O] > 750$ kJ mol$^{-1}$. In contrast to $UO_2^{2+}$ the second bond in O-$Pa^{2+}$-O is less than half as strong as the first—$D[OPa^{2+}\text{-}O] < 360$ kJ mol$^{-1}$—with the result that hydrolysis of hypothetical (formally hexavalent) $PaO_2^{2+}$(aq) to pentavalent $PaO(OH)^{2+}$(aq) is thermodynamically favorable.

Another interest in actinide oxide ions, particularly $AnO^+$, arises from their potential for illuminating the role of 5f electrons in molecular chemistry. From reactions of $An^+$ with alkenes via oxidative insertion, it was concluded that the 5f electrons of $Pu^+$, $Am^+$, $Cm^+$, $Bk^+$, $Cf^+$, and $Es^+$ do not directly participate in bonding in the {C-$An^+$-H} intermediates; rather, two non-5f electrons are needed for bond insertion.[6] To ascertain the participation of the 5f electrons in molecular bond activation for earlier actinides, where it is most plausible, we are systematically examining hydrocarbon activation by the oxo-ligated actinides, $AnO^+$. To a first approximation, two outer valence electrons at the metal center are engaged in formation of the $An^+$=O double bond. Thus, whereas the ground state of bare $U^+$ is $5f^37s^2$, that of $UO^+$ is $U^{3+}(5f^3)O^{2-}$.[7] Among the $AnO^+$ ions (An = Th, Pa, U, Np, Pu, Am, and Cm), $PaO^+$ exhibits a distinctive and remarkably high propensity to activate hydrocarbons by an oxidative insertion type of mechanism, which implies a {C-Pa-H} intermediate even after attachment of an O-atom to $Pa^+$.

The relatively inert character of $UO^+$ and heavier $AnO^+$ suggests that the 5f electrons at their metal centers are ineffective at oxidative insertion. To understand the distinctive reactivity of $PaO^+$ requires knowledge of its electronic structure. The ground state of bare $Pa^{3+}$ is $5f^2$, but this does not necessarily indicate that the ground state of $PaO^+$ is $Pa^{3+}(5f^2)O^{2-}$. The formal representation of fully ionic bonding in $PaO^+$ (and other $AnO^+$) is unrealistic: the bonding is undoubtedly substantially covalent. If the ground and low-lying electronic states of $PaO^+$ are (formally) $Pa^{3+}(5f^2)O^{2-}$, $Pa^{3+}(5f6d)O^{2-}$ or $Pa^{3+}(5f7s)O^{2-}$, the reactivity of $PaO^+$—i.e., the evident insertion of the Pa metal center into C-H bonds concomitant with formation of two bonds—would indicate participation of 5f electrons in organometallic bond activation. It is anticipated that theoretical calculations currently in progress at Ohio State University (R. M. Pitzer and R. Tyagi) will reveal the electronic structure of $PaO^+$.

*This work was supported by the U. S. Department of Energy, Office of Basic Energy Sciences under contract DE-AC05-00OR22725 with ORNL; and by Fundação para a Ciência e a Tecnologia under contracts POCTI/35364/QUI/2000 and POCTI/QUI/58222/2004. M. Santos is grateful to FCT for a PhD grant.*

1 H. H. Cornehl, C. Heinemann, J. Marçalo, A. Pires de Matos, and H. Schwarz, Angew. Chem. Int. Ed. Engl. **35**, 891 (1996).
2 J. K. Gibson, R. G. Haire, M. Santos, J. Marçalo, and A. Pires de Matos, J. Phys. Chem. A **109**, 2768 (2005).
3 L. V. Moskaleva, S. Krüger, A. Spörl, and N. Rösch, Inorg. Chem. **43**, 4080 (2004).
4 G. A. Shamov and G. Schreckenbach, J. Phys. Chem. A **109**, 10961 (2005).
5 M. Santos, A. Pires de Matos, J. Marçalo, J. K. Gibson, R. G. Haire, R. Tyagi, and R. M. Pitzer, *submitted to*: J. Phys. Chem. A (2006).
6 J. K. Gibson, Int. J. Mass Spectrom. **214**, 1 (2002).
7 J. Paulovič, L. Gagliardi, J. M. Dyke, and K. Hirao, J. Chem. Phys. **122**, 144317 (2005).

# Neptunyl V disproportionation and cation-cation interactions in organic solutions

**M.J. Sarsfield, R.J. Taylor, C.J. Maher, and R.B. Jarvis.**

**Nexia Solutions, Sellafield, Cumbria, CA13 1PG**

## INTRODUCTION

Neptunium can exist in a variety of formal oxidation states (+3 to +7), the most common form being the pentavalent neptunyl ion $[NpO_2]^+$.[1] Understanding the often intricate chemistry of $[NpO_2]^+$ is of fundamental importance to understanding neptunium behaviour under reprocessing, environmental and repository conditions.

It is well understood that pentavalent neptunyl ions are capable of disproportionation to Np(IV) and Np(VI) ions, particularly under conditions of high temperature, strong complexing ligands and high acidity in aqueous solutions. For example, in nitric acid the rate of reaction is described by the equation: $-d[Np(V)]/dt = 2k[Np(V)]^2[H+]^2$ where $k = 0.113 \pm 0.005$ $M^{-3}.min^{-1}$ at 90°C and $\mu = 4$ compared to $k = 0.07$ $M^{-3}.min^{-1}$ at 90°C and $\mu = 5$ in perchloric acid [2, 3].

These kinetics are considered slow with respect to other redox reactions and play a minor role in controlling neptunium routing under conditions relevant for reprocessing within the PUREX process. There is considerably less information concerning the disproportionation kinetics of neptunium in the organic phase (tributyl phosphate (TBP) + diluent). Here we examine how $[NpO_2]^+$ behaves when it is generated in a 30% TBP/odourless kerosene (OK) organic phase by UV/visible/near-IR and Raman spectroscopy.

## KEY OBSERVATIONS

Aqueous solutions of Np(VI) in nitric acid (0.1 – 2.5 M) are extracted in to the organic phase and chemically reduced to Np(V) ($[Np(V)] = 0.001 – 0.033$ M; $[H_2O] = 0.4$ M). The decrease of the 978 nm absorption maximum for $Np(V)_{org}$ was followed spetrophotometrically in the NIR region, with the rate of decrease depending on [Np], $[HNO_3]_{org}$ and temperature. The decrease in [Np(V)] is accompanied by an increase in absorption peaks associated with $Np(IV)_{org}$ and $Np(VI)_{org}$. In addition, we report the first evidence supporting the formation of a Np(V)---Np(IV) cation-cation interaction.[4] A summary of the reactions is given below and spectroscopic data have been fitted to this model. The results strongly support a disproportionation reaction and indicate a substantial increase in the rate of disproportionation compared to aqueous systems. Solvation effects on the rates and mechanism of disproportionation will be discussed.

The stability of cation-cation complexes of Np(V) with Np(IV), Np(V) and Np(VI) in the organic phase compared to previous studies in aqueous systems will also be addressed.

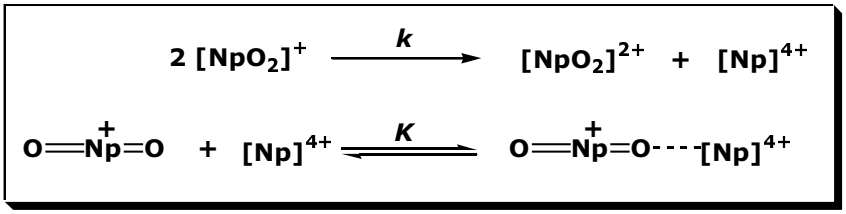


*Acknowledgements. Nexia Solutions and the Nuclear Decommissioning Authority for financial support.*

[1] J.J. Katz , G.T. Seaborg, L. Morss, Chemistry of the Actinides, 2nd Ed.; Chapman and Hall, London, (1986).
[2] V.S. Koltunov and M.F. Tikhonov, *Radiokhimiya*, **17**, 560, (1975).
[3] H. Escure, D. Gourisse and J. Lucas, *J. Inorg. Nucl. Chem*., **33**, 1871, (1971).
[4] J.C. Sullivan, A.J. Zielen, J.C. Hindman, J. Am. Chem. Soc. **82,** 5288, (1960), N.N. Krot and M.S. Grigoriev Russ. Chem. Rev. **73,** 89, (2004).

# Investigation of Actinide Molecules by Coupling X-ray Absorption Spectroscopy and Quantum Chemistry

C. Fillaux[*], C. Den Auwer[*], D. Guillaumont[*], D. K. Shuh[†] and T. Tyliszczak[†], J. C. Berthet[‡]

[*]CEA Marcoule, DEN/DRCP/SCPS, 30207 Bagnols sur Ceze Cedex, France
[†] Lawrence Berkeley National Laboratory, Berkeley, CA, USA
[‡] CEA Saclay, DSM/DRECAM/SCM, 91191 Gif sur Yvette Cedex, France

Both structural and electronic properties of the actinide cations are of fundamental interest in order to describe the intramolecular interactions. The *5f* and *6d* orbitals are the first partially or totally vacant states of these elements and their properties reflect the nature of the actinide-ligand bond. Because of its chemical and orbital selectivities, x-ray absorption near edge structure (XANES) spectroscopy is useful to probe the actinides' frontier orbitals and then understand the cation reactivity towards chelating ligands. It can provide information about the valency, the unoccupied electronic states and the effective charge of the absorbing atom.

The $L_3$-edge x-ray absorption spectroscopy of uranium (formal *2p-6d* transition in the dipolar approximation) has been the most reported one in the literature because of its convenient energy (17.2 keV). Although significant structural information on the coordination polyhedron can be obtained from these electronic transitions because of the important shape resonances[1,2], the very short core-hole lifetime broadens the edge signal (~7 eV) resulting in very little extractable electronic information. On the other hand, the $M_5$ (*3d-5f* transition) and $N_5$ (*4d-5f* transition) edges provide a better resolution (~4 eV for $M_5$ and $N_5$ core holes) and allow to achieve quantitative information.

In a preliminary work[3], multiple-edge approach has been proven fruitful in order to extract both structural and electronic properties of actinide compounds from XANES experimental spectra. Furthermore, we showed that coupling simulations of the experimental spectra and quantum chemical calculations lead to quantitative information such as the determination of the uranium coordination sphere and its effective charge.

In this work, XANES spectra are reported at the cation $L_3$, $M_{4,5}$, $N_{4,5}$ and $O_{4,5}$ thresholds and used to determined structural and electronic properties of actinide compounds. In addition, ligand *K*-edge spectra are analysed in order to better characterize the nature of the actinide-ligand bond.
Experimental data analysis by simulating the absorption edge allows to compare the coordination polyhedrons, identify the electronic transitions and calculate the density of states associated with the absorption spectra. Moreover, a coupling between simulations of the experimental spectra and quantum chemical calculations is performed, in order to improve the model describing the final states and better understand the bonding properties of the cation with the ligand.

An overview of the XANES spectra of $UO_2(NO_3)_2.6H_2O$ obtained at the various thresholds investigated is given in Figure 1; the spectra are plotted on a common relative energy scale.

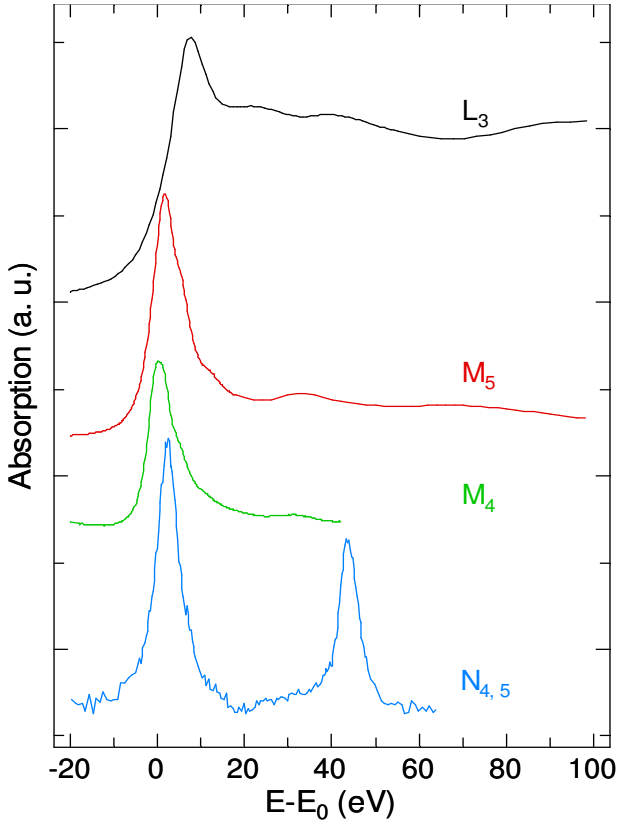


Fig 1: Near-edge x-ray absorption fine structure spectra of $UO_2(NO_3)_2.6H_2O$ at the $L_3$, $M_5$, $M_4$ and $N_{4,5}$ thresholds of uranium.

Analysis of experimental data, using the above mentioned method, will be shown for $UO_2(NO_3)_2.6H_2O$ and other actinide compounds.


1 R. Denning, J. Green, T. Hutchings, C. Dallera, A.Tagliaferri, K. Giarda, N. Brookes and L. Braicovich, J.Chem. Phys., **117**, 8008 (2002).

2 C. Den Auwer, D. Guillaumont, P. Guilbaud, S. D. Conradson, J. J. Rehr, A. Ankudinov, E. Simoni, New J. Chem., **28**, 929 (2004).

3 C. Fillaux, C. Den Auwer, D. Guillaumont, E. Simoni, N. Barré, D. K. Shuh and T. Tyliszczak, «Studies of Structural and Electronic Properties of Uranium Compounds, by XANES Spectroscopy», *MRS Boston 2005*.

# Tandem Mass Spectrometry and Wavelength-resolved Infrared Multiphoton Dissociation Studies of Gas-phase Uranyl Complexes

Michael Van Stipdonk[1*], Winnie Chien[1], Gary Groenewold[2], Anita Gianotto[2], Garold Gresham[2], Anita Gianotto[2], Jos Oomens[3], Nick Polfer[3], David Moore[3], Wibe de Jong[4], Lucas Visscher[5]

[*1]Department of Chemistry, Wichita State University, Wichita KS, USA
[2]Department of Chemical Sciences, Idaho National Laboratory, Idaho Falls ID, USA
[3]FOM Institute voor Plasmafysica "Rijnhuisen", Niewegein, The Netherlands
[4]Pacific Northwest National Laboratory, Richland WA, USA
[5]Vrije Universiteit Amsterdam, Amsterdam, The Netherlands

## INTRODUCTION

Reprocessing of nuclear fuel will require advanced separations of lanthanide and actinide elements beyond current capabilities. This necessity has motivated continued study of the structure and bonding of actinide and lanthanide ligand complexes, which in solution is often difficult to explicitly deduce because of varied and dynamic influences of the surrounding solvent. Difficulties with solution-phase characterization of actinide chemistry have spurred extensive research in computational chemistry. Mass analysis of complexes in the gas-phase greatly reduces the complexity, by providing explicitly defined compositions, but offers no direct structural information. Infrared multiphoton dissociation (IRMPD) of mass-selected complexes was used here to provide structural analysis of several gas-phase uranyl complexes, which enabled direct comparison with theoretical results.

## EXPERIMENTAL METHODS

Experimental measurements of vibrational spectra were conducted at the FOM Instituut voor Plasmafysica, "Rijnhuisen" in Niewegein, The Netherlands. Ions were generated by electrospray ionization (ESI) using established protocols [1, 2]. Spray solutions were composed of uranyl nitrate in deionized water, with 1-25% organic modifier such as acetonitrile, acetone, methylacetamide or dimethylformamide. The organic modifier became the coordinating ligand in the gas-phase uranyl complexes generated by ESI. Once formed, the complexes were trapped and isolated in a Fourier transform ion cyclotron resonance mass spectrometer. The complexes were irradiated with light from the free-electron laser, a continuously source of infrared radiation which was scanned from approximately 600 to 1800 $cm^{-1}$ in the experiments described here. Ion dissociation was observed when the laser was scanned through a resonance absorption band of the various uranyl complexes.

## RESULTS

Electrospray ionization of solutions of the uranyl dication containing organic co-solvents generated ligand (L) complexes having the general formula $[UO_2(L)_n]^{2+}$ where $1 < n < 5$. Complex ions fragmented by elimination of L when the laser wavelength was scanned through an absorption band. IRMPD of these complexes produced a diagnostic band corresponding to the uranyl asymmetric stretching frequency that was recorded between 1030 $cm^{-1}$ and 980 $cm^{-1}$. The O=U=O frequency systematically shifted to lower values as the number of electron-donating

ligands (n) in the complex increased (figure 1). For example, when L = acetone, this frequency red-shifted from 1017 $cm^{-1}$ to 988 $cm^{-1}$ as n was increased from 2 to 4, consistent with a modest weakening of the U=O bonds with increased number of coordinating ligands. Similar patterns were observed when L = acetonitrile, but the asymmetric stretching frequencies were ca. 20 $cm^{-1}$ higher relative to analogous complexes containing acetone. The difference in position of the asymmetric O=U=O shift for acetone and acetonitrile complexes with the same extent of ligation, are consistent with, and provide a direct measure of, the difference in nucleophilicity of the ligands bound to the uranium metal center. The experimentally measured asymmetric stretching frequencies compare well to values produced by ab-initio calculations [3] (figure 2.).

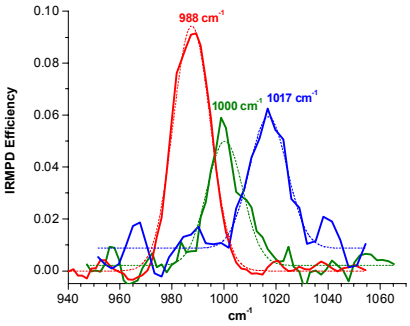


Figure 1. O=U=O stretch region of $[UO_2(acetone)_n]^{2+}$, where blue is n = 2, green is n = 3, and red is n = 4.

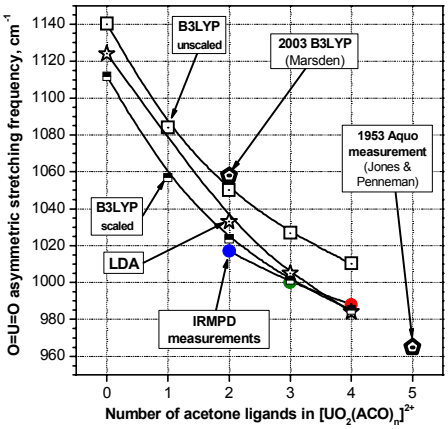


Figure 2. O=U=O stretch frequencies v. extent of ligation, measurements and calculations.

By varying the desolvation temperature used to generate the gas-phase complexes, ions containing $UO_2^+$ and $UO_2^{2+}$ with the same extent of ligation were produced, which allowed a direct measurement of the difference in O=U=O asymmetric stretching frequencies for analogous complexes containing U(V) and U(VI). For complexes containing the ligands methylacetamide or dimethylformamide (DMF), the asymmetric stretching frequency was ca. 100 $cm^{-1}$ lower for the U(V) complex compared to the U(VI) complex. The stretching frequency measured for "bare" species such as $[UO_2OCH_3]^+$, $[UO_2OH]^+$ and $[UO_2OOCCH_3]^+$ were 967, 970 and 990 $cm^{-1}$, respectively, consistent with a formal oxidation state of VI for U.

We have shown that complex ions containing $UO_2^+$, with general formula $[UO_2(L)_n]^+$ (where n=2, 3) will reversibly bind molecular $O_2$ [4]. IRMPD of complex ions with and without the pendant $O_2$ molecule demonstrate that the asymmetric O=U=O stretch of $[UO_2(DMF)_2]^+$ blue-shifts by ca. 60 $cm^{-1}$ upon $O_2$ addition, consistent with oxidation of $UO_2^+$ to $UO_2^{2+}$ and reduction of $O_2$ to $O_2^-$.

*This work is supported by the Department of Energy, Environmental Systems Research Program, the National Science Foundation and the Netherlands Organization for Scientific Research.*

1 M. J. Van Stipdonk *et al*., J. Phys. Chem. A. **108**, 10448-10457 (2004).
2 M. J. Van Stipdonk *et al*., J. Phys. Chem. A. **110**, 959-970 (2006).
3 G. S. Groenewold et al.; J. Am. Chem. Soc. (2006) accepted for publication.
3 G. S. Groenewold et al.; J. Am. Chem. Soc. (2006) Web Release: 2/11/2006; DOI: 10.1021/ja0573209.

# Atomistic Level Relativistic Quantum Modelling of Plutonium Hydriding

K. Balasubramanian, Thomas E. Felter, Tom Anklam, Thomas W. Trelenberg, and William McLean II

Lawrence Livermore National Laboratory, University of California, Livermore CA 94550 USA

## SUMMARY

The objective of our work is to develop and apply computational models to study corrosion of plutonium and uranium primarily through the hydriding process. We have developed and applied high level relativistic quantum chemical models to study the hydriding of plutonium. We have accomplished through atomistic level modelling by considering the interaction of a cluster of plutonium and plutonium atoms and ions with the hydrogen molecule: $H_2$. Our studies of $PuH_n$ for a variety of charges and sizes reveal that once $PuH_2$ or $PuH_3$ is formed it catalyzes further hydriding by forming a complex with $H_2$ and dissociating it without energy barrier. We show the computed Laplacian of the charge densities for various species considered in our study. To illustrate, the Laplacian map of $PuH_3$ in Fig 1shows a high peak on the plutonium site which suggests high propensity of the plutonium site in the hydrided form to remove the electronic charge density from another $H_2$ molecule thus breaking the $H_2$ bond so as to cause spontaneous further corrosion.

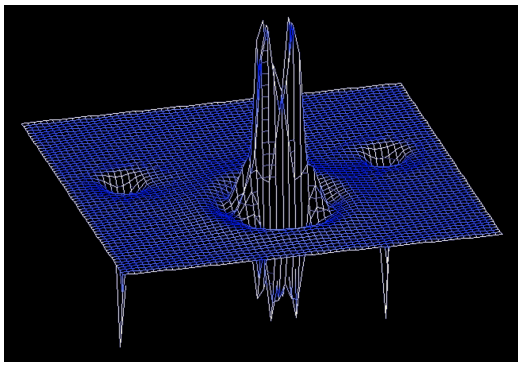

Fig.1 Lapalacian Charge Density of $PuH_3$ shows a high peak at Pu suggesting that Pu is very active in removal o fcharge desity from $H_2$ to catalyze further hydriding.

## COMPUTATIONAL METHODS

All of the computations reported here were carried out using high-level first principle (*ab initio*) computations that included both relativistic effects and electron correlation effects for Pu. We started with relativistic effective core potentials (RECPs) for Pu that replaced all but the outermost 16 electrons in the core, and have employed a variety of techniques from low-level (DFT/B3LYP) to high-level relativistic complete active space multi-configuration interaction self-consistent filed (CASSCF) and relativistic configuration interaction (RCI) computations. The potential energy surfaces

were computed using clusters of Pu interacting with $H_2$ as a function of $H_2$ approach and $H_2$ distance. We included several orientations for the potential energy surface, and the most favourable one was studied further at higher level of theory. These computations have included the important relativistic effects for Pu and the electron correlation effects. Thus this is the first study of its kind that introduces both relativistic and electron correlation effects to high degree in modelling Pu hydriding. We have generalized our codes and capabilities so that they can handle up to 70 million electronic configurations.

**RESULTS**

We have computed the stable equilibrium geometries, activation energy barriers, potential energy surfaces and Laplacian charge densities for plutonium hydride clusters, $PuH_n$ as a function of the size. Our computations on larger $PuH_n$ reveal that they are partially dissociated $H_2$ complexes of either $PuH_2$ or $PuH_3$. For example Fig 2 shows our computed equilibrium geometry of $PuH_4$. As seen from Fig.2, $PuH_2$ forms a complex with $H_2$ without a barrier due to the high propensity of Pu in $PuH_2$ to remove the electronic charge density from $H_2$ and dissociate the $H_2$ bond. This is fully consistent with the Laplacian charge density plot of $PuH_2$ shown in Fig. 3 which reveals a high peak on Pu suggesting that Pu is active in the removal of charge on $H_2$ and spontaneously attaching to $H_2$ and elongating the bond so as to cause dissociation. Our computations on $PuH_5$ also reveal that it is a $PuH_3$ + $H_2$ complex formed without an energy barrier.

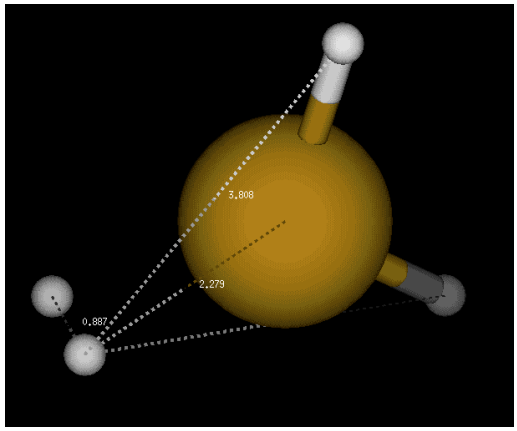


Fig 2: Computed Equilibrium Geometry of $PuH_4$ shows that it is a complex of $PuH_2$ with a partially dissociated $H_2$ thus catalyzing further hydriding.

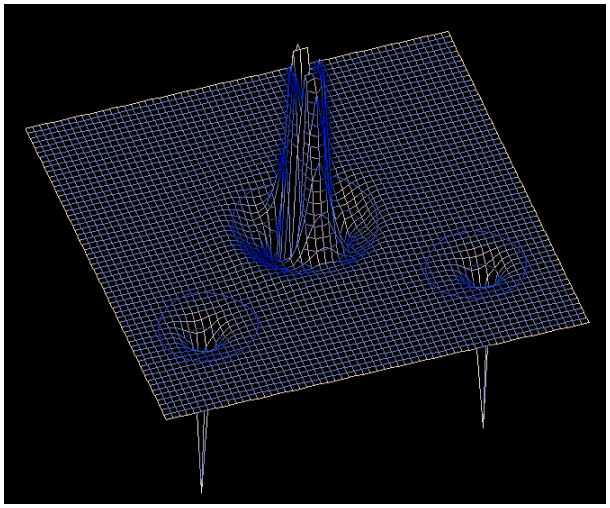

Fig 3 Lapalcian of $PuH_2$ shows that the high peak on Pu would actively bind to other $H_2$ molecules without a barrier.

*Acknowledgements* *This work was performed under the auspices of the U.S. Department of Energy, by the University of California, Lawrence Livermore National Laboratory under contract No. W-7405-ENG-48.*

.

# Formation of Volatile Oxygen-Bearing Compounds by U, Np, Pu and Am

V.P. Domanov

Joint Institute for Nuclear Research, Dubna, Moscow reg., 141980, Russia

## INTRODUCTION

The results of the work on obtaining volatile oxygen-bearing compounds of uranium and plutonium are summarized. A distinctive property of the performed experiments is the use of actinide-containing samples that served as a source for generation of volatile products. The method of their production is presented. It is based on collection of recoil atoms emitted from a solid actinide target, transformation of the collected atoms into a chemically active form, for example, hydrides, and subsequent transfer of the hydrides onto the surface of a quartz powder.

The other features of the performed experiments were described earlier[1,2]: they were carried out using the thermochromatographic (TC) method and open quartz TC columns; oxygen was used as a reagent and helium served as a carrier gas; the gas mixture was purified from impurities; the initial sample contained tracer quantities of actinide to be studied; it was placed in the starting zone of the TC column and was heated in the gas steam at 700-750°C; forming volatile compounds were adsorbed at certain temperatures of the thermogradient (TG) section of the TC column. After completing each experiment the TG section was cut into equal portions and their inner surface was treated with a suitable solvent . The α-sources were prepared from the solutions obtained. They were measured using an α-spectrometer that consisted of a silicon surface barrier detector and corresponding electronic units.

Recent experiments with neptunium and americium have been carried out in similar conditions.

## URANIUM

It was found that natural uranium (1-2μg was used in each experiment) formed three volatile compounds that were adsorbed at 450±25°C, 250±25°C and 120±25°C in a stream of dry gas. The thermochromatogram obtained was deciphered by using the results of model experiments. It was shown that uranium was deposited in the form of dioxide in the first zone, the second zone was connected with adsorption of $UO_3$ and the third zone was formed due to uranium acid adsorption (assumed $H_2UO_4$). The values of adsorption enthalpy $-\Delta H_a^0$ for $UO_2$ and $UO_3$ on quartz were calculated. They were equal to 172±6 kJ.mol$^{-1}$ and 126±6 kJ.mol$^{-1}$ respectively.

## PLUTONIUM

The initial sample contained $10^9$-$10^{10}$ atoms of $^{238}$Pu or $10^{11}$-$10^{12}$ atoms of $^{239}$Pu. Formation of four adsorption zones was registered in the experiments with plutonium. Their centers were located at 450±30°C, 250±30°C,130±50°C and at the negative temperature −105±25°C. Model experiments with $^{185}OsO_n$ (n=2,3,4) were performed for the interpretation of the composition of vol atile plutonium forms. Chemical behavior of the isolated compounds was also studied in a large interval of oxygen concentration $C_{O_2}$ (in helium) from $10^{-6}$ to 50% (vol.). As a result, it was shown that $PuO_2$ was adsorbed in the first zone, $PuO_3$ was deposited in the second zone and the last zone was formed through adsorption of very volatile octovalent plutonium in the form of $PuO_4$.

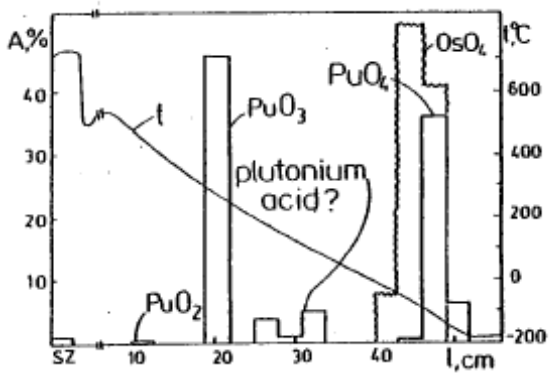


Fig 1: Termochromatogram of volatile plutonium compounds at $C_{O_2}$ =50%.

The calculated values of $-\Delta H_a^0$ for isolated plutonium oxides on quartz were equal to 175±7 kJ.mol$^{-1}$ ($PuO_2$), 122±7 kJ.mol$^{-1}$ ($PuO_3$) and 47±8 kJ.mol$^{-1}$ ($PuO_4$). The third zone was evidently formed through adsorption of plutonium acid (assumed $H_2PuO_4$).

The mass spectrometric measurements performed by Ronchi et al.[3] confirmed occurrence of $UO_2$, $UO_3$, $PuO_2$ and $PuO_3$ in the gas phase.

Distribution of plutonium compounds along the TC column is shown in Fig. 1. For comparison of volatilities of Pu and Os tetraoxides the adsorption zone of $^{185}OsO_4$ is also shown.

**NEPTUNIUM**

Formation of volatile neptunium oxides was expected prior to the performance of the experiment. Based on the values of $-\Delta H_a^0$ for U and Pu oxides on quartz, the value of $-\Delta H_a^0$ should be equal to 173±7 kJ.mol$^{-1}$ for $NpO_2$ and 125±7 kJ.mol$^{-1}$ for $NpO_3$. Trace quantities of $^{237}Np$ ($10^{12}$-$10^{13}$ atoms) were used in each experiment. They were performed at $c_{O_2}$=50% and $c_{O_2}$=1%. Figure 2 shows the neptunium distribution along the TC column at $c_{O_2}$=50%. Its α-activity was found at 400-450°C, 220-270°C and 30-90°C. The relation between the first and second peaks was in favor of the second peak here. Three adsorption peaks were also observed at $c_{O_2}$=1% and they were registered at the same temperatures, but the relation between the first and second peaks was reverse.

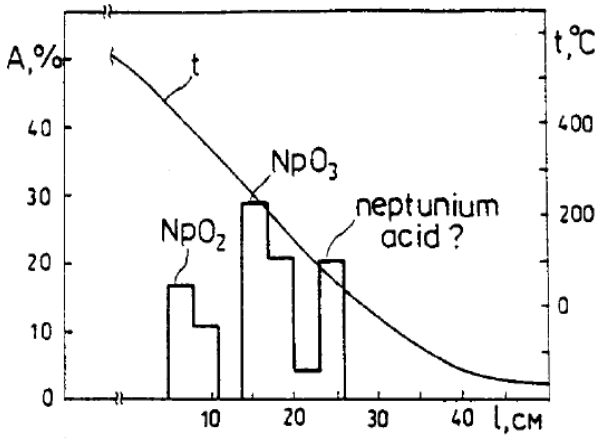

Fig 2: Thermochromatogram of volatile neptunium compounds at $c_{O_2}$=50%

Thus, it was shown that the first peak was formed by $NpO_2$ deposition and the second peak was formed by $NpO_3$ adsorption. Based on the experimental data, the values of $-\Delta H_a^0 NpO_2$=167±6 kJ.mol$^{-1}$ and $-\Delta H_a^0 NpO_3$=124±6 kJ.mol$^{-1}$. These values agree with our estimates of adsorption enthalpy for $NpO_2$ and $NpO_3$. The third adsorption peak might be due to formation of neptunium acid (assumed $HNpO_4$).

**AMERICIUM**

The experiments with $^{243}Am$ were a sort of probing. The initial sample contained $10^{10}$ to $10^{11}$ atoms of $^{243}Am$. Three adsorption peaks were registered at $c_{O_2}$=50%. They were located at 500±25°C, 330±25°C and 160°C. Similar distribution of α-activity along the TC column was obtained in the experiments with U and Np. Based on this, it can be assumed that the first peak was formed through $AmO_2$ deposition, the second was connected with $AmO_3$ adsorption and americium acid forms the third peak. The values of $-\Delta H_a^0$ for the supposed oxides were calculated. They were equal to 180±7 kJ.mol$^{-1}$ ($AmO_2$) and 144±7 kJ.mol$^{-1}$ ($AmO_3$). The calculated values are higher than those for U, Np and Pu oxides. These differences do not contradict the known concept. Noting the similarity of physical and chemical properties of U, Np, Pu and Am in a certain valence state, Haissinsky[4] explained that "these properties change gradually with increasing atomic number, i.e. with decreasing atomic radius".

Thus, a sound assumption has been made that the isolated oxides have chemical compositions $AmO_2$ and $AmO_3$, and the most volatile compound was americium acid (presumably $H_2AmO_4$).

References

1 V.P. Domanov, *et al.*, Radiokhimiya. **44**, 106, (2002) (in Russian).
2 V.P. Domanov, *et al.*, J. Nucl. Sci. Technol. Suppl. 3, 579, (2002).
3 C. Ronchi, *et al.*, J. Nucl. Mater. **280,** 111, (1996).
4 M. Haissinsky, *et al.*, in the book: Radiochemical Survay of the Elements, Amst./Lon./N.Y., Elsevier Publish. Comp., p. 164, (1965)

# Structures and Bonding in $K_{0.91}U_{1.79}S_6$ and $KU_2Se_6$

H. Mizoguchi[*], D. L. Gray[*], F. Q. Huang[*,†], J. A. Ibers[*]

[*]Department of Chemistry, Northwestern University, Evanston IL 60208 USA
[†]Shanghai Institute of Ceramics, Shanghai 200050 PR China

The compounds $K_{0.91}U_{1.79}S_6$ and $KU_2Se_6$, members of the $AAn_2Q_6$ actinide family ($A$ = alkali metal or Tl; $An$ = Th or U; $Q$ = S, Se, or Te), have been synthesized from $US_2$, $K_2S$, and S at 1273 K and U, $K_2Se$, and Se at 1173 K, respectively. $KU_2Se_6$ shows Curie-Weiss behavior above 30 K and no magnetic ordering down to 5 K. The value of $\mu_{eff}$ is 2.95(1) $\mu_B$/U. Its electronic spectrum shows the peaks characteristic of f-f transitions. It is a semiconductor with an activation energy of 0.27 eV for electrical conduction. Both $K_{0.91}U_{1.79}S_6$ and $KU_2Se_6$ crystallize in space group *Immm* of the orthorhombic system and are of the $KTh_2Se_6$ structure type[1]. Both contain infinite one-dimensional linear $Q-Q$ chains characteristic of the $AAn_2Q_6$ family. Typical of the known $AAn_2Q_6$ compounds, in $KU_2Se_6$ there are two alternating Se–Se distances of 2.703(2) Å and 2.855(2) Å, both much longer than a Se–Se single bond. In contrast, in $K_{0.91}U_{1.79}S_6$, the first sulfide of this family to be characterized structurally, there are alternating normal $S_2^{2-}$ pairs 2.097(5) Å in length. In $K_{0.91}U_{1.79}S_6$ the formal oxidation state of U is 4+.

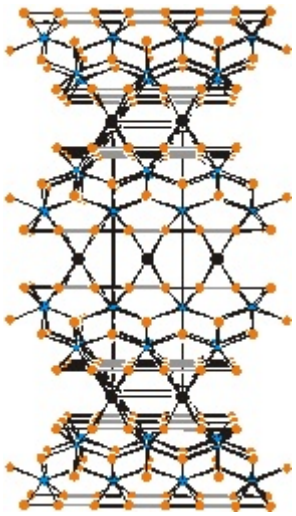

Fig. 1: Structure of $KU_2Se_6$ viewed down [100].

$K_{0.91}U_{1.79}S_6$ can be thought of as K insertion into $US_3$, leading to the series $K_xU_{2-x/4}S_6$ ($1 \geq x \geq 0$). The structure of $US_3$ ($x = 0$), determined from a single-crystal X-ray diffraction study[2], will be compared with those of $K_{0.91}U_{1.79}S_6$ and $KU_2Se_6$.

*Research kindly supported by the U. S. Department of Energy, Grant ER-15522.*

1 K.-S. Choi, R. Patschke, S. J. L. Billinge, M. J. Waner, M. Dantus, and M. G. Kanatzidis, J. Am. Chem. Soc. 120, 10706-10714 (1998).

2 J. Kwak, D. L. Gray, H. Yun, and J. A. Ibers, to be published (2006).

# Electron Spectroscopy Study of Pu and Pu Compounds

T. Gouder

European Commission, Joint Research Centre, Institute for Transuranium Elements, Postfach 2340, 76125 Karlsruhe

Study of the electronic structure of Pu and its alloys has to face the complex nature of the *5f* states, between localized and itinerant. Over the last 20 years, photoelectron spectroscopy has been used to obtain information on the density of states (DOS) of Pu. Yet, it is not a ground state technique, and in highly correlated systems, final state effects occur, making direct comparison of spectra with the ground state DOS difficult. Current interpretation of photoemission data is therefore controversial, and ranges from direct comparison with ground state DOS calculations [1, and references therein] and an novel mixed level model, stating that part of the *5f* states are localized, and part itinerant [1]. We will present a somewhat different interpretation in terms of narrow band ground state, with typical final state effects (multiplets, screening) produced by the photoemission process itself. We will compare Pu with its surrounding actinide elements (U, Np, Am) and show, that Pu is not exotic but its photoemission spectra are consistent with those of the other actinides.

After ejection of the photoelectron the atom is left in an ionized state, and for the early actinides this results in two types of final state effects. The first is associated with the screening of the photohole. If the f-states are well hybridized, they perform the screening. But upon *f*-localization, alternative screening (*ds*-screening) becomes active. At the localization threshold the two screening types coexist. This results in spectral satellites, which have no correspondence in the ground state DOS. Such satellites can be well identified by performing core-level spectroscopy (*4d*, *4f* states). Because core levels are intrinsically sharp and well defined, any supplementary satellites point to final state effects. For Pu such core-level satellites are so common, that also for valence band spectra their existence has to be anticipated. The peculiarity in studying the *5f*-states by photoemission is that photoelectron and screening electron are from the same (*f*) level. In well itinerant system this simply means, that the final state is identical to the ground state (refilling of the photohole). But when the *f*-hybridization becomes weak, the lifetime of the photohole may become so long, that in the time frame of the experiment, it behaves as localized hole. This leads to the second final state effect, the existence of final state multiplet structures. They are generally observed in localized systems (e.g. rare earths) [2]. We claim that even in weakly itinerant systems multiplets are observed, because the final state photohole is not immediately filled. Combination of the two final state effects accounts for many

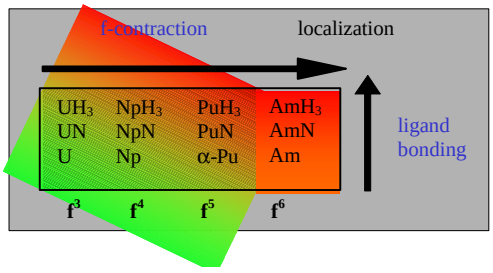


*Fig. 1 5f localization/delocalization in early actinide compounds.*

of the spectroscopic features in Pu compounds: starting from a $f^n$ initial state, two final states ($f^n$ and $f^{n-1}$) are reached and appear with their characteristic multiplet structures.

We will discuss this by placing Pu in the context of the other early actinides (Fig. 1) and investigate, how correlation and final state effects appear with gradual *5f* localization, when passing from the mostly *5f* itinerant U, to Np, Pu and eventually Am, where the *5f* states are localized. Metals are compared with simple compounds (nitrides, hydrides), where itinerancy of the *5f* states is further modified by bonding interaction with ligand states. In compounds, hybridization with *f*-states favours *5f* itinerancy, whereas partial removal of *ds* states (oxidation) and increase of actinide-actinide inter-atomic distance favours localization. Which of the opposing effects prevails, depends on the type of compound. For all actinides, hydrides are more localized than nitrides. Consistently, for the hydrides the $f^{n-1}$ final state is more pronounced than for the nitrides ($f^n$). In $PuH_3$ and PuN, the three *ds* states participate in the bonding, leaving Pu with a $5f^5$ configuration (Fig. 2). Photoemission of an *f*-electron leads to the $f^4$ ionized intermediate state, which depending on the type of screening either returns to the $5f^5$ configuration (*f*-screening) or remains as $5f^4$ (*ds*-screening). The corresponding multiplets have been calculated, based on optical spectroscopy data [3], fit well the experimental curves. Even in α-Pu, which is the most itinerant of all Pu-allotropes, satellite structures appear between 0-1 eV binding energy, and become more pronounced in δ-Pu. They show strong similarity with the $5f^5$ final state multiplet structure. Similar satellites are also observed in Pu silicides, and again interpreted in terms of $5f^5$ and $5f^4$ multiplets [4].

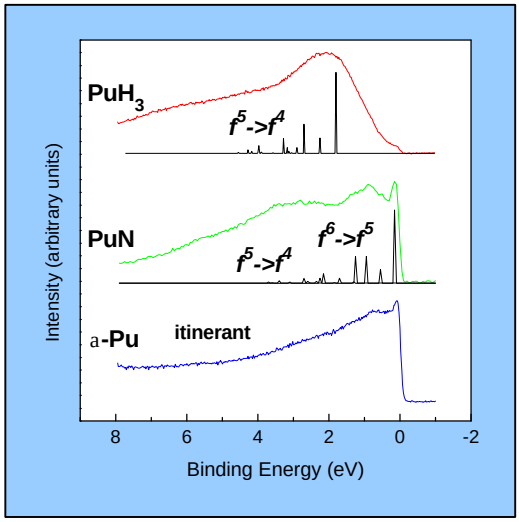


*Fig. 2 Valence band photoemission spectra of a-Pu, PuN and $PuH_3$.*

Another interesting class of Pu compounds are the chalcogenides (PuSe [5] and PuTe). These are intermediate valence systems, with a well localized $5f^5/5f^6$ ground state configuration. Photoemission from these compounds leads to the corresponding $5f^4/5f^5$ final state multiplet structures, which always represent the ds-screened final state. Here, coexistence of the multiplets is not a final state effect (the *f*-states are well localized) but reflects true ground state mixing.


1 J.M. Wills, *et al.*, J. Electron. Spectros. Relat. Phenom. 135 (2004), 163.
2 M. Campagna, G.K. Wertheim, and Y. Baer, Photoemission in Solids II, Case Studies, Photoemission in Applied Physics Vol. 27 (Springer Verlag, Berlin, 1979).
3 F. Gerken and S. Schmidt-May, J. Phys. F: Met. Phys. **13**, 1571 (1983).
4 T. Gouder, *et al.*, Phys. Rev. B **71**, 165101 (2005).
5 T. Gouder, *et al.*, Phys. Rev. Lett. **84**, 3378 (2000).

# Competition Between Delocalization and Spin-Orbit Splitting in the Actinide 5*f* States[#]

James G. Tobin

[*]Lawrence Livermore National Laboratory, Livermore CA 94552 USA
Email: Tobin1@LLNL.Gov

## DISCUSSION

Synchrotron-radiation-based X-ray absorption, electron energy-loss spectroscopy in a transmission electron microscope, multi-electronic atomic spectral simulations and improved first principles calculations (Generalized Gradient Approximation in the Local Density Approximation, GGA/LDA) have been used to investigate the electronic structure of the light actinides: $\alpha$-Th, $\alpha$-U and $\delta$-Pu. It will be shown that the spin-orbit interaction can be used as a measure of the degree of localization of valence electrons in a material. The spin-orbit interaction in the light actinide metals, $\alpha$-Th, $\alpha$-U and $\delta$-Pu, has been determined using the branching ratio of the white line peaks of the $N_{4,5}$ edges, which correspond to 4d -> 5f transitions. Examination of the branching ratios and spin-orbit interaction shows that the apparent spin-orbit splitting is partially quenched in $\alpha$-U, but is strongly dominant $\delta$-Pu. These results are fully quantified using the sum rule. This picture of the actinide 5f electronic structure is confirmed by comparison with the results of electronic structure calculations for $\alpha$-Th, $\alpha$-U and $\delta$-Pu, which in turn are supported by a previous Bremstrahlung Isochromat Spectroscopy (BIS) experiment.

This work was performed under the auspices of the U.S. DOE by Univ. of California, Lawrence Livermore National Laboratory under contract W-7405-Eng-48.

[#]J.G. Tobin, K.T. Moore, B.W. Chung, M.A. Wall, A.J. Schwartz, G. van der Laan, and A.L. Kutepov, "Competition Between Delocalization and Spin-Orbit Splitting in the Actinide 5*f* States," Phys. Rev. B **72**, 085109 (2005).

# Microscopic theory of magnetism and superconductivity of Pu and $PuMGa_5$ on the basis of a j-j coupling scheme

Takashi Hotta*

*Advanced Science Research Center, Japan Atomic Energy Agency, Tokai, Ibaraki 319-1195, Japan

Recent high research activities on Pu-based materials in condensed matter physics have been triggered by the discovery of superconductivity in $PuCoGa_5$ with amazingly high transition temperature $T_c$=18.5K [1]. The superconductivity has been also found in $PuRhGa_5$ with $T_c$=8.7K [2, 3]. From Ga NMR and NQR measurements [4, 5], it has been confirmed that the gap function of $PuMGa_5$ has line-node structure with d-wave symmetry. In addition, Pu has also attracted renewed attention. In particular, recent μSR experiment has set the new limit for magnetic moment less than $10^{-3}\mu_B$ on δ-Pu [6], in spite of the theoretical prediction of magnetism to explain atomic volume expansion in δ-Pu. It is a challenging issue to understand the unconventional superconductivity with such high $T_c$ in Pu-based compound and the mechanism of the absence of magnetism in δ-Pu.

In order to develop microscopic theories of magnetism and superconductivity in f-electron compounds, recently we have proposed the construction of an f-electron model on the basis of a j-j coupling scheme [7]. The model contains the kinetic term of f electrons, Coulomb interaction term among f electrons, and the crystalline electric field potential for f electron. Using this model, we have explained spin and orbital structure of $UMGa_5$ [8] and $NpMGa_5$ [9]. Recently, octupole ordering in $NpO_2$ has been also understood from the microscopic viewpoint [10]. Encouraged by such successes of the j-j coupling model in actinide materials, we attempt to understand magnetism and superconductivity of Pu and $PuMGa_5$ by analyzing the model with the use of numerical and analytical techniques. For δ-Pu, we consider an fcc lattice, while for $PuMGa_5$, the model is set up on a two-dimensional square lattice. We focus on a key role of 5f orbital state for the appearance of superconductivity in $PuMGa_5$ and the absence of magnetism in δ-Pu.

*The work on $PuMGa_5$ has been done in collaboration with K. Kubo. We have been supported by Grants-in-Aid from the Ministry of Education, Culture, Sports, Science, and Technology of Japan and the Japan Society for the Promotion of Science.*

1 J. L. Sarrao et al., Nature **420**, 297 (2002).
2 F. Wastin et al., J. Phys.: Condens. Matter **15**, S2275 (2003).
3 Y. Haga et al., J. Phys. Soc. Jpn. **74**, 1698 (2005).
4 N. J. Curro et al., Nature **434**, 622 (2005).
5 H. Sakai et al., J. Phys. Soc. Jpn. **74**, 1710 (2005).
6 R. H. Heffner et al., Physica B, in press.
7 T. Hotta and K. Ueda, Phys. Rev. B **67**, 104518 (2003).
8 T. Hotta, Phys. Rev. B **70**, 054405 (2004).
9 H. Onishi and T. Hotta, New J. Phys. **6**, 193 (2004).
10 K. Kubo and T. Hotta, Phys. Rev. B **71**, 140404(R) (2005); *ibid.* **72**, 144401 (2005); *ibid.* **72** 132411 (2005).

# On the Absence of Magnetic Order in Plutonium

J. C. Lashley[*], A. C. Lawson[*], R. McQueeney[€], and G. H. Lander[†]

[*]Los Alamos National Laboratory, Los Alamos New Mexico, 87545 USA
[€] Ames Laboratory & Dept. of Physics Iowa State University Ames, Iowa 50011 USA
[†]European Commission, JRC, Institute for Transuranium Elements, Postfach 2340 Karlsruhe, Germany

Plutonium exhibits many states with relatively small energy differences between them. In practice it has proven difficult to calculate, measure, or to know its ground state under various conditions. In many related heavy fermion materials and dilute alloys, electrons at low pressure exhibit behaviour intermediate between weak and strong electron-electron correlation. A satisfactory theoretical description of electrons in this regime has not been found [1]. Theorists are in the position of having the interacting Dirac hamiltonian without being able to isolate the part of the theory that controls the behaviour of electrons. Consequently a chemist finds many valence states, while a metallurgist finds competing crystal structures and large volume changes between them, and physicists find that computational tools fail to give what we have observed - sometimes we wondered where the *f* -electrons went.

Electronic energy band calculations and electron-photoemission, positron annihilation, and Compton scattering measurements of δ-plutonium showed that the *f*-electrons were always there but somehow their contributions to the binding energy could be switched on and off. But when it was switched off, why could the localized *f*-electron not be found? A partial answer is that the light actinide series is characterized by a transition of the electronic structure from itinerant to localized 5*f* behaviour with an increasing complexity that culminates in δ-plutonium. This effect is seen clearly in the evolution of the electronic specific heat [2,3] across the actinides as shown in Fig. 1.

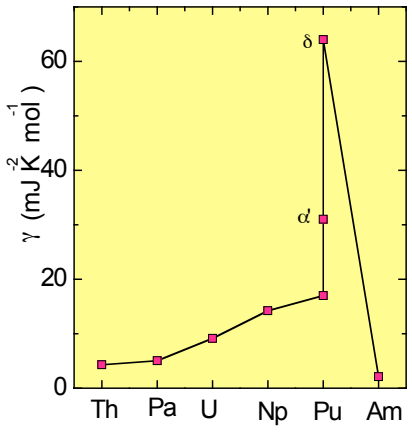


Figure 1. Evolution of γ across the actinides.

In the dense Pu phases, which have low crystallographic symmetry, the 5f electrons in Pu are thought to participate in bonding, similar to the 3d orbitals in the transition metals giving rise to electronic specific heats of 20 mJ $K^{-2}$ $mol^{-1}$. The low-symmetry structures have been attributed to Peierls instabilities associated with the transition of electronic structure in the 5*f* series. Conversely, the low-density phases (obtained by alloying) have high crystallographic symmetry and the 5*f*-orbitals are thought to be more localized, similar to the 4*f*-orbitals in the rare earths showing enhanced electronic specific heats. However unlike the rare earths, there is no experimental evidence for a pronounced local magnetic moment associated with the 5*f* state in the low-density metals. Here we review the experimental situation the experiments presented

and discussed are magnetic susceptibility, electrical resistivity, NMR, specific heat, and both elastic and inelastic neutron scattering. We comment on the fact that many recent calculations correctly predict experimentally observed atomic volumes, including that of δ-Pu. These calculations achieve observed densities by the localization of electrons, which then give rise to magnetic moments. However, localized magnetic moments have never been observed experimentally in Pu and the latest muon spin experiments [4] have set a small lower limit on any ordered moment. Dynamic experiments showing emergent moments (e.g., alterations in the lattice due to self-irradiation damage) will be discussed within this context. Finally, recent heat capacity and photoemission results in Am-stabilized δ-Pu are also discussed with regard to the around-mean-field LSDA+U correlated band theory [5].


[1]. M. Boring and J. L. Smith, Los Alamos Science
[2]. J.C. Lashley, A. C. Lawson, R. McQueeney and G. H. Lander, Phys Rev B., **72** 054416 (2005).
[3]. B. Mihaila et. al., Phys. Rev. Lett. **96,** 076401 (2006).
[4]. R. H. Heffner et al. ArXiv:cond-mat/0508694
[5]. A. Shick et. al. Phys. Rev. B., **73**, 1 (2006).

# Self-Damage and Magnetic Susceptibility in Pu and Pu alloys as a Probe of the 5*f* electrons

S.K. McCall, M.J. Fluss, B.W. Chung, G.F. Chapline, M.W. McElfresh, R.G. Haire, D.J. Jackson
Lawrence Livermore National Laboratory, Livermore CA 94550 USA

*Abstract*

The 5*f*-electrons of both α-Pu and δ-Pu occupy a narrow *f*-band as indicated by the large magnitudes of both the electronic specific heat and Pauli (temperature independent) magnetic susceptibility. While some theoretical models of Pu accurately predict the energy-volume relationship of the various Pu phases, they require non-vanishing magnetic moments, yet there are no experimental measurements indicating any sort of localized moments in the "pure" metal[1, 2]. However the narrow *f*-band suggests that Pu is nearly magnetic, and should display evidence of magnetic moments given an appropriate perturbation.

The Hill conjecture postulates that within the actinides magnetism or its absence is determined primarily by the actinide separation[3]. For plutonium compounds, a separation greater than 3.4A should produce magnetic moments. Indeed, this is observed for fluorite structured $PuH_2$, where the Pu atoms retain an FCC structure akin to the δ-phase, with the hydrogen atoms effectively acting as spacers to stretch the Pu-Pu distance to 3.79A, leading to local moments (~1$\mu_B$/Pu) that antiferromagnetically order at 30K[4]. Similarly, a Pu atom in isolation is expected to have a local moment arising from the incomplete 5*f* shell, and one way to approximate this is to dissolve small quantities of Pu in a non magnetic lattice such as Pd. Instead of forming the simple local moments of a Kondo impurity as was observed for dilute Np in Pd, Pu acts like a local spin fluctuation system with a characteristic temperature, $T_{sf}$ ~ 1K and an effective moment of 1$\mu_B$/Pu[5]. Similarly, dilute doping of Pu into La sharply decreases $T_c$ in contrast to doping Am into La which has a minimal impact on $T_c$[6]. This again implies a magnetic state for the Pu atoms when individual atoms are isolated within a non-magnetic lattice.

The converse of the above doping experiments would be to remove or displace isolated Pu atoms from a regular

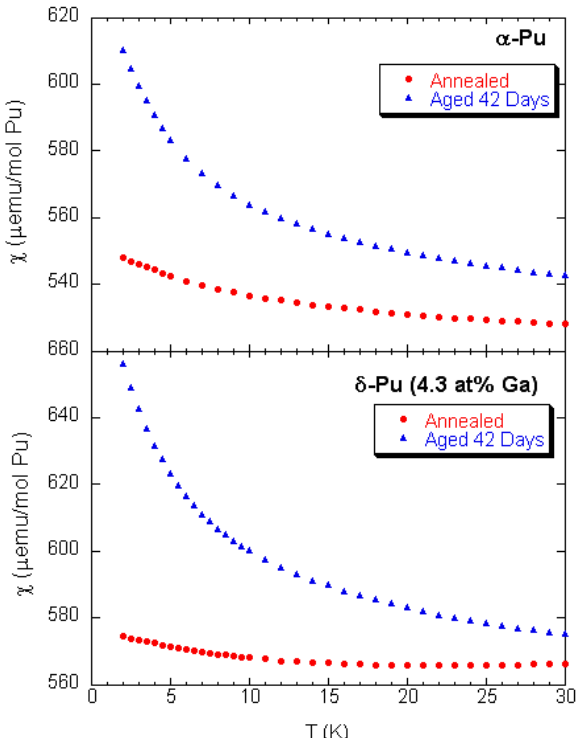


**Fig. 1 Magnetic susceptibility taken at 3T**

lattice, effectively doping with vacancies and/or interstitials, and observe what, if any, influence this has on the magnetic properties. Pu decays by emission of a 5 MeV alpha particle with a corresponding 86 keV U recoil, generating a damage cascade of ~2500 vacancies and interstitials. Most of these immediately recombine, but a few hundred defects remain, and at sufficiently low temperatures (T< 35K), they become frozen within the lattice. In other words, at low temperatures Pu dopes itself with vacancies (and interstitials). This damage is observable as an increase in the magnetic susceptibility with time (damage) that returns to the undamaged initial (t=0) value after annealing to 350K and consistent with earlier resistivity measurements [7]. Thus the excess magnetic susceptibility (EMS) arises from the defects, and not the decay products which are unaffected by thermal annealing. The EMS is strongly temperature dependant, as shown in Fig. 1 for annealed and representative 42-day damaged curves, thereby suggesting there are evolving localized spins and hinting at characteristics of the 5*f* electrons hidden in the undamaged material.

*This work was performed under the auspices of the U.S. Department of Energy by University of California, Lawrence Livermore National Laboratory under Contract W-7405-Eng-48.*

[1] P. Soderlind, and B. Sadigh, Phys. Rev. Lett. **92**, 185702 (2004).
[2] J. C. Lashley *et al.*, Phys. Rev. B **72**, 054416 (2005).
[3] H. H. Hill, in Plutonium 1970 and Other Actinides, edited by W. N. Miner (Metall.Soc. and Amer. Inst. Mining, 1970), p. 2.
[4] A. T. Aldred *et al.*, Phys. Rev. B **19**, 300 (1979).
[5] M. B. Brodsky, Rep. Prog. Phys. **41**, 1547 (1978).
[6] H. H. Hill *et al.*, Physica **55**, 615 (1971).
[7] M. J. Fluss, et al., J. Alloys Compd. **368**, 62 (2004).

# Influence of interstitial impurity and vacancy on δ-Pu magnetic state: *ab-initio* investigation

M.A. Korotin[*], A.O. Shorikov[*], V.I. Anisimov[*], V.V. Dryomov[†], Ph.A. Sapozhnikov[†]

[*]Institute of Metal Physics, 620041 Ekaterinburg GSP-170, Russia
[†]RFNC-VNII Technical Physics named after acad. E.I. Zababakhin, Snezhinsk, Russia

## INTRODUCTION

Results of magnetic properties investigation for *pure* metallic Pu published in last year have promoted the modern idea of nonmagnetic ground state of plutonium in δ and α phases. This rather unexpected conclusion follows from both the complex analisis of experimental data[1] and the results of band structure caluclations[2,3] in frames of improved methods with the proper regard for exchange and spin-orbit couplings of Pu *5f*-electrons.

However it is difficult to accept the statement about the absence of magnetism in Pu, especially for experimentalist community, since available Pu samples always demonstrate the traces of magnetic interactions. What are the reasons for their appearance?

We continue to popularize the idea of nonmagnetic ground state of metallic plutonium adducing the hypothesis about formation of magnetism in it due to the presence of defects and arguing this hypothesis by new results of our band structure calculations.

## APPROACH

For our investigation we have used the so-called *LDA+U+SO* band structure calculation method. It is based on the Local Density Approximation (*LDA*) including Coulomb (*U*) and Spin-Orbit coupling (*SO*) in *a generalized matrix form*. Such modification of standard *LDA* is caused by comparable strength of exchange and spin-orbit interactions happened in actinides. Just competition, or delicate balance between these two types of interactions determines the nonmagnetic state of the 5*f*-shell of Pu. The details of the *LDA+U+SO* method and calculation results for plutonium in δ and α phases without defects could be found elsewhere[3].

Due to construction, the *LDA+U+SO* method is appropriate for the investigation of non-collinear magnetics. Starting the self-consistency loop from arbitrary (e.g. ferro) magnetic order, new mutual orientation of spins corresponding to the minimal total energy will be obtained at the end.

## CRYSTAL STRUCTURE MODEL

A supercell consisting of *32 Pu atoms* originally arranged in the positions of δ phase *plus* interstitial Pu impurity in one of the octa-holes of FCC lattice *plus* vacancy (in fact, minus one Pu) in the third coordination sphere of the imputity was constructed. With the use of molecular dynamics Modified Embedded Atom Model (*MEAM*), the atomic positions were relaxed inside this supercell.

## VALUES FOR COULOMB, EXCHANGE AND SPIN-ORBIT CONSTANTS

In addition to atomic numbers and atomic positions in the supercell, the values of on-site Coulomb ($U$), exchange ($J_H$) and spin-orbit coupling constants ($\lambda$) for *5f*-shell of Pu are input parameters in the *LDA+U+SO* method. All three of them were found[3] to be $U$ =2.50 eV, $J_H$ =0.48 eV, $\lambda$=0.31 eV.

## RESULTS

As it was calculated earlier[3], the metallic Pu in δ phase has a nonmagnetic ground state with Pu ions in $f^6$ configuration with zero values of spin (***S***), orbital (***L***), and total (***J***) moments. The *5f*-band is split by spin-orbit coupling into well-pronounced $f^{5/2}$ subshell filled with six electrons and empty $f^{7/2}$ subband (see Fig. 1).

The presence of interstitial impurity together with vacancy leads to the appearance of weak magnetism. This result agrees well with recent experiments[4] confirmed the presence of sizeable magnetic moments in aged Pu samples, which however disappear after annealing. Magnetic order obtained in our calculations is presented in Fig.2.

The physical reason for magnetic solution is polarization of the Pu *5f*-shell due to the slight filling of $f^{7/2}$ subshell (originally empty in pure Pu) and corresponding decrease of $f^{5/2}$ subshell filling (Fig. 1) caused by crystal structure distortions. The averaged value of effective paramagnetic moments per Pu atom in the supercell,

.

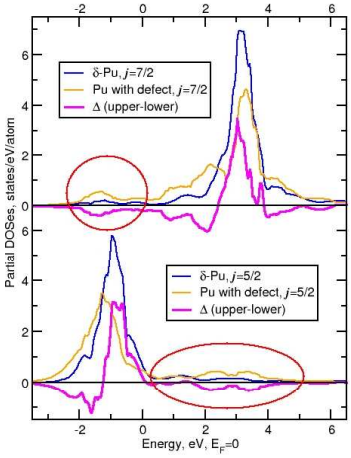


Fig. 1. Projected density of *5f*-states for pure δ Pu (blue lines), defect Pu (orange lines) and their difference (magenta lines). Most informative energy ranges are marked by red ellipses. Negative difference inside upper ellipse means the higher contribution of defect Pu $f^{7/2}$ states to the occupied spectral interval. Negative difference inside lower ellipse means the higher contribution of defect Pu $f^{5/2}$ states to the unoccupied spectral interval, i.e. their devastation.

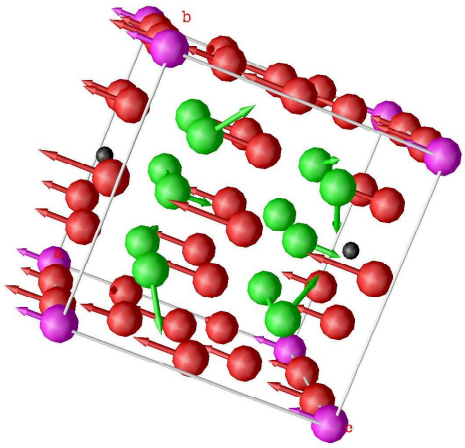


Fig. 2. Calculated magnetic structure for Pu supercell with interstitial atom (magenta balls) and vacancy (black balls). Arrows show directions of ***J***, green and red colours correspond to different signs of $J_z$ component. Length of arrows is proportional to $\mu_{eff}$.

$\mu_{eff} = g\sqrt{J(J+1)}\mu_B$, is calculated to be $\mu_{eff}$=0.18 $\mu_B$. The absolute values of moments vary within $0.02 \le S \le 0.27$, $0.03 \le L \le 0.36$, $0.01 \le J \le 0.11$.

Interstitial impurity and vacancy influence on the values of magnetic moments in different ways. As we have investigated, the interstitial impurity alone polarizes the *5f*-shell of neighboring atoms the more, the farther they are. The vacancy alone brings opposite tendency: the nearest neighbors possess maximal moments and the latter decrease with distance. Together, two types of defects compensate each other more or less, providing weak magnetism of defect plutonium.

There is one more interesting aspect of the results. Whereas the interstitial impurity alone forms ferrimagnetic order close to AFM A-type inside the supercell, the vacancy alone changes this order to C-type. Acting simultaneously, they produce non-collinear magnetic structure shown in Fig. 2 due to the competition of influences of defects.

## CONCLUSIONS

Basing on the *LDA+U+SO ab-initio* calculations we have demonstrated that while pure Pu is nonmagnetic, the defects of Pu crystal such as interstitial impurity and vacancy could be responsible for weak magnetism revealing in various experiments. The calculated value of effective paramagnetic moment is in reasonable agreement with experimental estimates[4].

*M.A.K. acknowledges Russian Science Support Foundation.*

1 J.C. Lashley, A. Lawson, R.J. McQueeney, and G.H. Lander, Phys. Rev. B **72**, 054416 (2005).
2 A.B. Shick, V. Drchal, and L. Havela, Europhys. Lett. **69**, 588 (2005).
3 A.O. Shorikov, A.V. Lukoyanov, M.A. Korotin, and V.I. Anisimov, Phys. Rev. B **72**, 024458 (2005).
4 S.K. McCall, M.J. Fluss, B.W. Chung, D.J. Jackson, G.F. Chapline, and M.W. McElfresh, submitted to Phys. Rev. Lett. (UCRL-JRNL-217097, 11 Nov 2005).

# The effect of exact calculation of exchange interaction upon calculated electronic structure of actinides

A.L. Kutepov

Institute of Technical Physics (VNIITF), Snezhinsk, Russia

**ABSTRACT**

Electronic and magnetic structure of plutonium and americium has been investigated within relativistic Hartree-Fock approach (Dirac-Fock). The calculations have been conducted with new developed Dirac-Hartree-Fock linear muffin-tin orbital method. In this full-potential method the Metfessel's idea of interpolation was applied to calculate coulomb and exchange integrals and to represent density and potential in the interstitial region.

Calculated within Hartree-Fock approach the electronic structure appears to be in a great disagreement with the electronic structure calculated within density functional theory (GGA) (Fig.1).

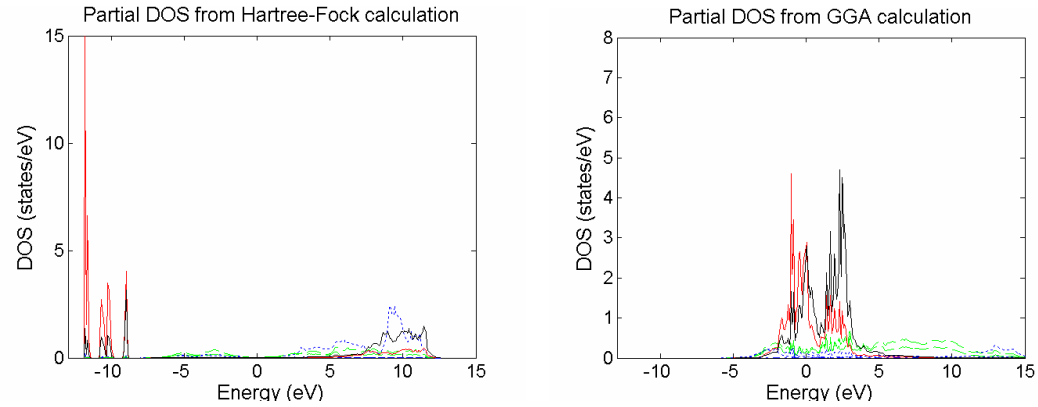


Fig.1. Partial DOS of ferromagnetic fcc Pu as obtained in Hartree-Fock calculation (left) and in GGA calculation (right). Red color – $5f_{5/2}$. Black – $5f_{7/2}$.

The orbital dependence of the potential in Hartree-Fock method leads to a strong splitting between filled and empty f-bands. Despite the obvious disagreement with experiment (which, however, can be easily explained by absence of screening and other correlation effects in the present Hartree-Fock calculations) the results obtained let us draw some conclusions.

1) It is clear that LDA(GGA) completely fails in describing of the exchange in actinides. This fact can be seen from the following considerations. In view of the fact that Hartree-Fock calculation (i.e. exact treatment of exchange interaction) leads to zero DOS at Fermi level, the experimental peak of DOS at Fermi level can be explained only as coming from dynamical correlation effects. But correlation in LDA has nothing common with this peak (the LDA calculation without correlation (exchange only) give the same picture of DOS as LDA with correlation). Thus, the peak of DOS at Fermi level in LDA is noting else as a consequence of

some approximations in calculating of the exchange interaction. So, the success of LDA in describing of the above peak and obviously connected with it the success in describing of the equilibrium properties, can be just attributed to some happy fortuity.

2) It is interesting, however, that electronic configuration of the ground state of ferromagnetic plutonium is $5f^5$ in Hartree-Fock calculation (as it is in LDA(GGA) calculation) with nonzero spin and orbital magnetic moments. Total energy of nonmagnetic $5f^6$ configuration, which is the ground state in the LDA+U calculations (references [1] and [2]), appeared to be much higher in present Hartree-Fock calculations than total energy of $5f^5$ configuration. Thus we have magnetic $5f^5$ configuration in two different methods (Hartree-Fock and LDA(GGA)), which contradicts with nonmagnetic $5f^6$ obtained with LDA+U approach. This difference can be explained either by absence of screening in the present Hartree-Fock calculations or by inadequacy of LDA+U Hamiltonian (which clearly is not obtained ab initio) for studying of plutonium electronic structure. So, this question has to be studied further.

3) Apparently, this work can serve as some evidence of the fact that electronic structure of actinides can be described only within some many-body picture, like DMFT. But, applying the DMFT one should be careful, using LDA+U as a starting point (which is common approach presently).

1. Shick, A. B., Drchal, V. & Havela, L. Coulomb-*U* and magnetic moment collapse in d-Pu. Europhys. Lett. **69**, 588 (2005).
2. Shorikov A.O., Lukoyanov A.V., Korotin M.A., and Anisimov V.I., Phys Rev B **72,** 024458 (2005).

# Actinyl Chemistry across the U, Np and Pu series

S.M. Cornet*, I. May*, M.J. Sarsfield†, N. Kaltsoyannis‡, J. Haller‡

* Centre for Radiochemistry Research, Department of Chemistry, The University of Manchester, Manchester M13 9PL, UK
† Nexia Solutions, BNFL Technology Centre, Sellafield, Seascale,Cumbria, CA20 1PG, UK
‡Department of Chemistry, University College London, 20 Gordon Street, London WC1H, UK

## INTRODUCTION

A better understanding of the behaviour of the mid-actinides elements (U, Np, Pu and Am) is necessary for effective radioactive waste management and environmental remediation. The linear dioxo cations, $AnO_2^{x+}$ (x=1 or 2), dominate the +V and +VI oxidation state chemistry for these actinides, with between 4-6 additional ligands in the equatorial plane. Among the series, the uranyl moiety $\{UO_2\}^{2+}$ has been studied extensively. Our recent studies have focused on soft N donor ligands which have shown out of plane coordination, promoted U-C interaction and enhanced the Lewis basicity of the uranyl oxygen.[1-4] In contrast, due to higher radioactivity of the transuranic elements, there have been less studies on the transuranic actinyl cations. Although, Np(V) has been studied in depth for cation-cation complexation,[5] non aqueous Np(V) and Np(VI) chemistry remains comparatively unexplored due to the current lack of suitable precursor. Our current goal is to fill this gap and extent our investigations on O- and N-donor ligands to $NpO_2^{2+}$ and $PuO_2^{2+}$.

## EXPERIMENTAL FACILITIES

Our route into N-donor complexes of $\{UO_2\}^{2+}$ has been through the thf complex $[UO_2Cl_2(thf)_3]$,[6] enabling the manipulation of the cation under inert, moisture free conditions, using standard Schlenk line and dry box procedures. Our initial attempts to prepare the Np analogue have thus far proved unsuccessful. Although $NpO_2Cl_2(R_3PO)_2$ has proved to be a good starting material for preparing novel neptunyl phosphinimine complexes.[7] However, the presence of moisture in the system can result in the hydrolysis of the phosphinimine ligands to a chloride salt $R_3PNH_2^+Cl^-$. All experiments were carried out in a negative pressure inert atmosphere glove box specially designed to work with high radioactivity material (Np). Access to the laboratories facilities at CEA, Atalante, Marcoule (France) will allow us to extent our research to plutonyl chemistry.

## COMBINED EXPERIMENTAL AND COMPUTATIONAL STUDIES

The displacement of phosphine oxide by phosphinimine ligands proved experimentally that $UO_2Cl_2(R_3PNH)_2$ and $NpO_2Cl_2(R_3PNH)_2$ are more stable than their phosphine oxide analogues. Solution NMR experiments suggest that *cis* and *trans* isomers exist which is surprising because the *cis* isomer would be expected to have greater steric repulsion between the bulky phosphinimine ligands. In order to gain further insight into these observations, relativistic, gradient corrected Density Functional Theory has been used to study these compounds. Total bonding energy calculations have been carried out to establish which of the *cis* or *trans* isomers is the most stable, both in gas-phase and in solution. Optimized geometries have been used to determine bond distances and angles and the strength of the U-N bond has been calculated

(using the fragment approach within ADF, and also through calculations of Mayer bond orders) and compared to the analogous U-O bond in the phosphine oxide complex. NMR chemical shifts of N-*H* have been calculated, in gas phase or $CD_2Cl_2$ solution. These computational studies will be extended to systems containing f-elements (Np and Pu complexes).

## CURRENT RESEARCH

The uranyl complex $UO_2Cl_2(Ph_3PO)_2$ has previously proved to be a successful precursor to prepared uranyl(VI) alkoxide complexes.[8] It has been shown that electron rich alkoxide ligands can enhance the basicity of the oxo groups on the uranyl moiety.[9] $NpO_2Cl_2(Cy_3PO)_2$ (See Fig 1) and $NpO_2Cl_2(Ph_3PO)_2$ would thus appear to be good starting for $\{NpO_2\}^{2+}$ alkoxide chemistry, continuing our investigation into f-electron containing actinyl species. The next step would be to study analogous $\{PuO_2\}^{2+}$ chemistry.

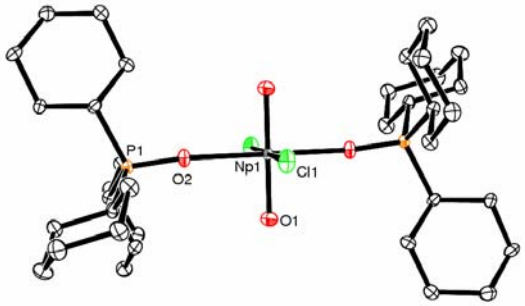


Fig 1: ORTEP representation of $NpO_2Cl_2(Cy_3PO)_2$

## CONCLUSIONS

Although non aqueous uranyl chemistry is well developed, non aqueous neptunyl and plutonyl chemistry is much less; carefully selected synthetic routes and specialist facilities are thus required to study such systems.


1 M. J. Sarsfield, M. Helliwell, and D. Collison, Chem. Comm., 2264 (2002).
2 M. J. Sarsfield, H. Steele, M. Helliwell, et al., Dalton Trans, 3443 (2003).
3 M. J. Sarsfield, M. Helliwell, and J. Raftery, Inorg. Chem. **43**, 3170 (2004).
4 M. J. Sarsfield and M. Helliwell, J. Am. Chem. Soc. **126**, 1036 (2004).
5 I. Charushnikova, Radiochemistry **46**, 565 (2004).
6 M. P. Wilkerson, C. J. Burns, R. T. Paine, et al., Inorg. Chem. **38**, 4156 (1999).
7 M. J. Sarsfield, I. May, S. M. Cornet, et al., Inorg. Chem. **44**, 7310 (2005).
8 C. J. Burns, D. C. Smith, A. P. Sattelberger, et al., Inorg. Chem. **31**, 3724 (1992).
9 M. P. Wilkerson, C. J. Burns, H. J. Dewey, et al., Inorg. Chem. **39**, 5277 (2000).

# Alpha spectrometry with high energy resolution cryogenic detectors

E. Leblanc[*], N. Coron[†], J. Leblanc[†], P. de Marcillac[†], J. Bouchard[*], M. Loidl[*]

[*]Laboratoire National Henri Becquerel, CEA Saclay, Gif sur Yvette Cedex 91191, France
[†] CNRS, Institut d'Astrophysique Spatiale, Orsay 91405, Cedex, France

## INTRODUCTION

Isotopic ratio determination of actinides is a major concern in the fields of nuclear fuel cycle, environment monitoring and health survey of workers potentially exposed to radioactivity. When high quality sources can be prepared, alpha spectrometry with conventional silicon detectors is an inexpensive method, therefore widely used. However, the energy resolution of these detectors is intrinsically limited and in some cases it does not allow to separate isotopes emitting radiation of close energies. Mass spectrometry is potentially a powerful alternative to radioactive decay counting in the qualitative detection of actinides. But in the case of complex compounds (Uranium and Plutonium), atomic isobars induce still unsolved difficulties[1].

For many applications, one would need an equipment with a resolving power of 1/1000 and excellent detection efficiency not as complex as a mass spectrometer. In order to pass the limit of conventional detectors, we have analysed what limits their energy resolution for alpha particles and we have conceived two different alpha detectors with a detection principle fundamentally different than the one of a conventional detector.

## A THERMAL DETECTOR WITH A COPPER ABSORBER AND A RESISTANCE THERMOMETER

Apart from the loss and spread of energy in the dead layer of a semiconductor detector, the main contribution to a degraded energy resolution is the statistical distribution between electron-hole pair production and nuclear recoils. The recoil energy will mainly be converted into heat which is not seen by a classical detector. Hence a thermal detector, operated at a very low temperature so that its heat capacity is small enough, should allow a very sensitive and precise measurement of alpha particle energy. This was demonstrated accidentally by Allessandrello[2] and Vanzini[3] with $^{210}$Po, an internal contaminant of their $TeO_2$ bolometer. However, a dielectric absorber is not an ideal material to conceive an alpha detector. One has to minimize all the possible loss of energy such as fluorescence emission and creation of lattice defects. A metal is more appropriate. But even at very low temperature, the heat capacity of a metal is so high that it is a challenge to build a sensitive and fast thermal detector. We have considered different geometries to optimise the thermal coupling between the different parts of the detector and used a copper absorber and a resistance thermometer (doped germanium).

We have measured external sources of Americium and Plutonium with a conventional silicon detector and with the bolometer described above and we have compared the results. For an external source, the energy resolution obtained with the copper bolometer is 5.5 keV for 5.5 MeV alpha particles (see Figure 1). The full width at half maximum (FWHM) of the Gaussian is 4 keV, which is to be compared to typically 8 keV in the case of conventional silicon detectors.

Fig 1: External $^{241}$Am source measured with a copper bolometer

(time of measurement: 12 hours)

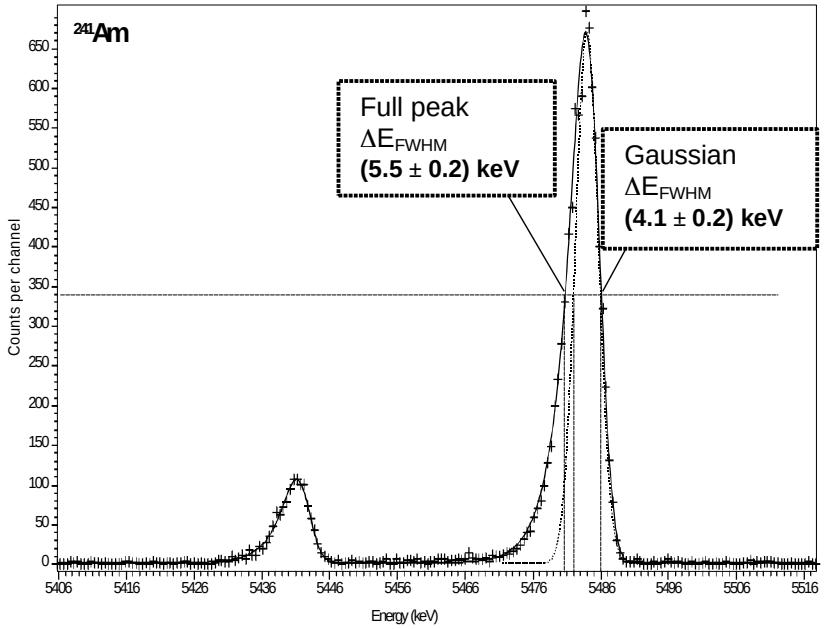


## OPTIMISATION OF SIGNAL LECTURE: A GOLD ABSORBER WITH A MAGNETIC THERMOMETER

Considering a metallic absorber, an even better choice for the thermometer is a paramagnetic metal alloy whose magnetisation in the presence of a magnetic field varies strongly with temperature. The change of magnetic flux following an alpha particle interaction can be read out with a very high sensitivity using a SQUID magnetometer. Detectors based on this principle, have been developed for X-ray spectrometry[4]. The challenge to conceive such a detector for alpha spectrometry is the requirement of a much larger absorber. We will present the concept of the detector and the signal read-out scheme.

*This experiment has been supported by LNE (Laboratoire National de Métrologie et d'Essais), the French Institute for Metrology and CNES (Centre National d'Etudes Spatiales).*

1 M.E. Ketterer et al., Journal of Environ. Radioact., 67 (3), 191-206 (2003).
2 A. Alessandrello, et al., Nuclear Instruments and Methods, A440, 397-402 (2000).
3 M. Vanzini, et al., Nuclear Instruments and Methods A461, 293-296 (2001).
4 C. Enss, et al., Journal of Low Temperature Physics 121, 137-176 (2000).

# PLUTONIUM SPECIATION
# BY ELECTROSPRAY MASS SPECTROMETRY

B. Amekraz, C. Moulin

CEA-DEN/DANS/DPC/SECR-Laboratory of Speciation of Radionuclides and Molecules, 91191 Gif sur Yvette, FRANCE.

Speciation of plutonium at low level is still a major challenge in the framework of environmental and biochemical studies in order to understand its behaviour. Owing to its different oxidation states as well as colloidal or polymeric forms, it is important to have sensitive and selective spectrometric methods to identify and quantify the different complex present in solution. Among them, Electrospray mass spectrometry (ES-MS) is a method of choice. First developed for biological applications since it allows for very high mass by making multicharged species, ES-MS is a powerful tool for speciation studies in solution due to its soft mode of ionization and has been used for speciation of lanthanides[1-3] and actinides such as uranium[4-5] and thorium[6] in interaction with different ligands of interest but never for plutonium. Hence, due to radioactivity, spraying plutonium in a mass spectrometer is not straightforward.

For the first time, a mass spectrometer equipped with a nanospray interface has been completely modified to be further integrated in a gloves box. This completely new device (see figure 1) has been used to look at different plutonium systems, from plutonium in acidic solution to plutonium in interaction with polycarboxilic acid such as EDTA for the characterisation of the different species present in solution and to evaluate the capabilities of such spectrometer for the speciation of plutonium with its different oxidation states. Comments on the built up of such spectrometer, capabilities of nanoES-MS for speciation as well as first results obtained for different plutonium solutions will be presented.

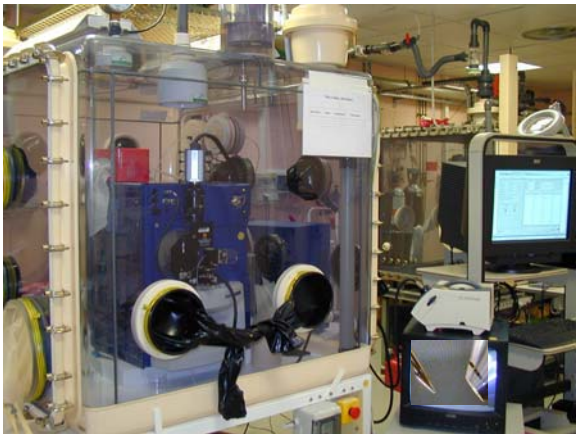

Fig 1 : NanoES-MS spectrometer in gloves box for Pu speciation

*Acknowledgements* : *The authors would like to thank DDIN/Risk assessment and DSOE/Basic Research for their financial support.*

1. C. Moulin, B. Amekraz, V. Steiner, G. Plancque, E. Ansoborlo, Appl. Spectro. **57**, 1151 (2003).
2. B. Amekraz, S. Colette, C. Madic , L. Berthon , G. Cote, C. Moulin, Inorg. Chem. **43**, 6745 (2004).
3. T. Vercouter, B. Amekraz, P. Vitorge, C. Moulin, Inorg. Chem **44**, 7570 (2005).
4. C. Moulin, N. Charron, G. Plancque, H. Virelizier, Appl. Spectro. 54(6), (2000).
5. C. Jacopin, M. Sawicki, G. Plancque, D. Doizi, F. Taran, E. Ansoborlo, B. Amekraz, C. Moulin. Inorg. Chem. **42**, 5015 (2003).
6. B. Amekraz, C. Moulin, S. Hubert, V. Moulin, Anal. Chim. Acta **441**, 269 (2001)

# Heat treatment effects on the surface chemisorption behavior of strained uranium: the $H_2O$/U reaction

E. Tiferet[†] M. H. Mintz[*,†], S. Zalkind[*], I. Jacob[†] and N. Shamir[*]

*Nuclear Research Centre-Negev, POB 9001, Beer-Sheva 84190, Israel
[†]Dept. of Nuclear Eng., Ben-Gurion Univ. of the Negev, POB 653, Beer-Sheva, 84104, Israel

The initial interaction of $H_2O$ vapor with polycrystalline uranium surfaces was studied with samples initially strained, then strain relieved by heat treatments, performed in the temperature range up to 700 K. The chemisorption characteristics of these surfaces were studied by a combination of direct recoils spectrometry, Auger electron spectroscopy and X-ray photoelectron spectroscopy.
Also X-ray diffraction measurements were used to determine the level of strain relief induced by each of the heat treatments.

Significant changes in the water-surface interactions were displayed for the different heat treatments. These changes were observed for both, the very initial chemisorption stage, taking place on the metallic clean surfaces and for the following stage, occurring on the fully oxidized surfaces. For example:
a) The initial sticking coefficient is heat treatment dependent (Fig. 1 vs. Fig. 2).

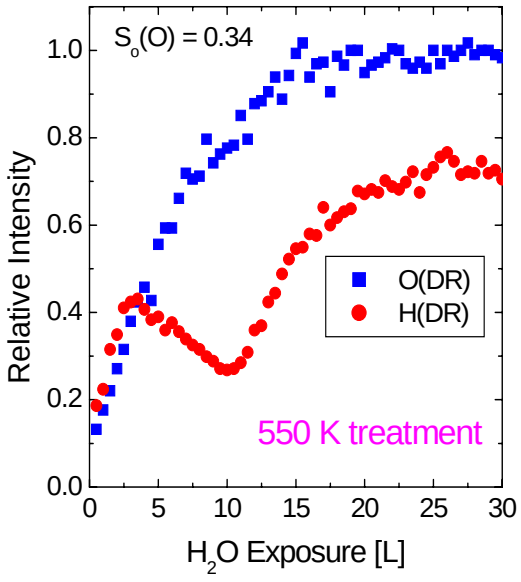


Fig. 1: O(DR) and H(DR) vs. $H_2O$ exposure for the 550 K heat treatment. The sticking coefficient was calculated from the "clustering" best fit.

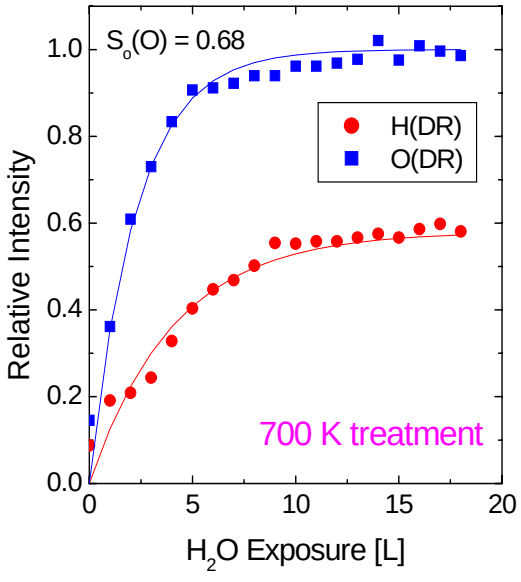


Fig. 2: O(DR) and H(DR) vs. $H_2O$ exposure for the 700 K heat treatment. The sticking coefficient was calculated from the "clustering" best fit (blue line).

b) For the former stage, a partial dissociation $H_2O$ molecule occurs on the as received sample and full dissociation occurs for the heat treated surfaces, with the clustering of the O's (or OH's) into island, independent on the heat-treatment. On the oxide, partial dissociation occurs also on the 450 K treated sample (Fig. 3), in contrast to full dissociation on the rest (Fig. 4).

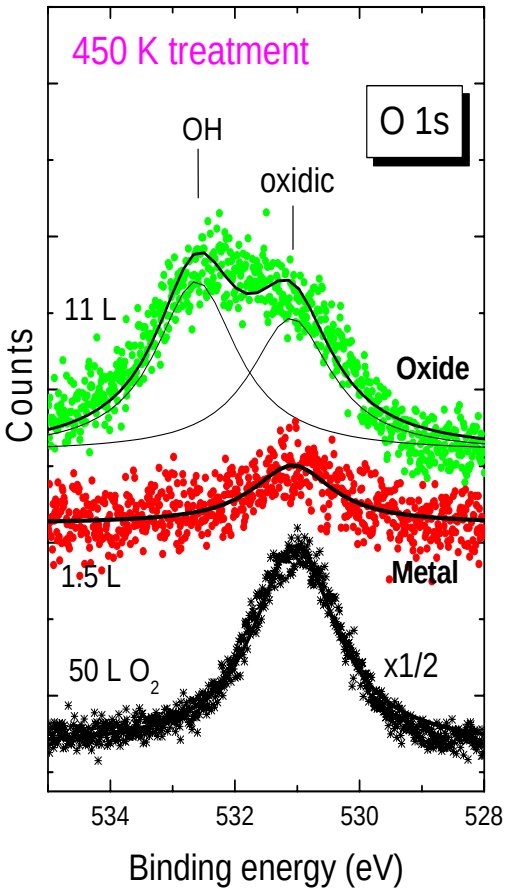


Fig. 3: O 1s XPS spectra of $H_2O$ adsorption (compared to $O_2$ adsorption) on the metallic and oxidized surfaces after a 450 K heat treatment.

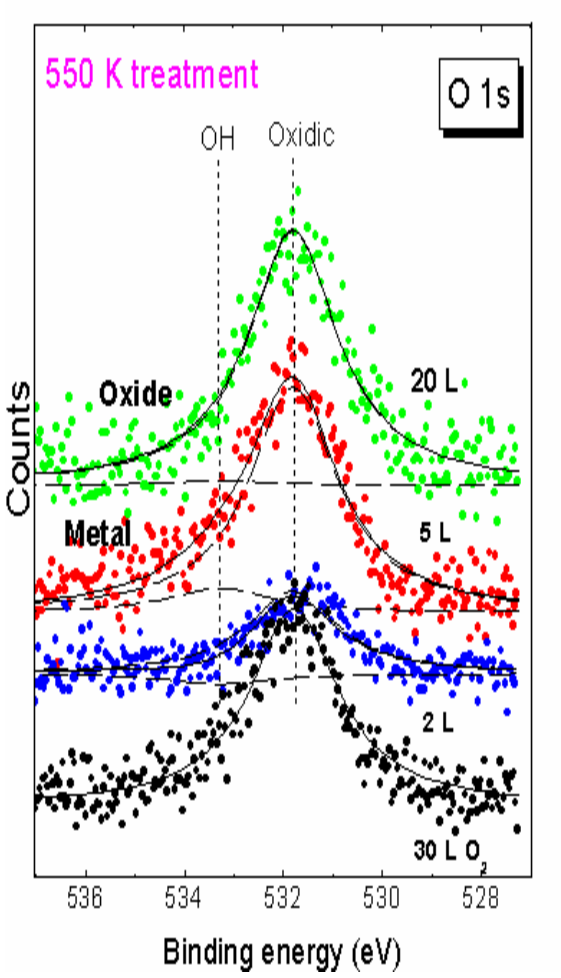


Fig. 4: O 1s XPS spectra of $H_2O$ adsorption (compared to $O_2$ adsorption) on the metallic and oxidized surfaces after a 550 K heat treatment.

c) The behavior of the chemisorbed dissociated H's is dependent on the heat-treatment temperature, changing from a random adatom distribution, occurring for the lower temperature treatment (Fig. 1), into an island clustering mechanism, displayed for the higher treatment one (Fig.2). The present article summarizes the previous results published on this system,[1,2] adds a large amount of new observations and presents an up-to-date whole picture of these heat treatment effects.


1 M. H. Mintz and N. Shamir, Appl. Surf. Sci., **252,** 633 (2005).

2 N. Shamir, E. Tiferet, S. Zalkind and M. H. Mintz, Surf. Sci., in press.

# A photoemission study of the oxidation of the light actinides

P. Nevitt[1], P. Roussel[2], T. Gouder[3], F. Huber[3] and A. Carley[1]

[1] School of Chemistry, Cardiff University, P.O. Box 912, Cardiff, CF10 3TB. U.K.
[2] AWE, Aldermaston, Berkshire. RG7 4US U.K.
[3] European Commission, Joint Research Centre, Institute of Transuranium Elements, Postfach 2340, D-76125, Karlsruhe, Germany.

When compared to the lanthanide elements, the light actinide's (thorium to americium) display remarkably different chemistry. Most lanthanide chemistry is restricted to the +3 oxidation state. The valence 4f electrons of the lanthanide elements appear mostly immune to perturbation by the metal coordination sphere and bonding is considered to be ionic in nature. In contrast, the valence 5f electrons of the actinide elements play a significant role in determining the physical and spectroscopic properties. This is because of the greater spatial extension of the 5f valence states of the light actinides verses the 4f states of the lanthanide elements. However, the degree on 5f electron interaction will decrease, relative to 6d interaction with increasing oxidation state and also vary with increasing atomic number. Thus, to investigate the effects of the 5f electron behaviour it would be ideal to undertake a systematic study of actinide elements. It should be noted that thorium, which has a $5f^0 6d^2 7s^2$ ground state acts a good comparison as an element that has no 5f electrons and its chemistry is dominated by the +4 oxidation state.

The electropositive nature of the light actinide elements, means the metal surfaces will always be covered with an oxide film. However, various methods of obtaining oxide free metallic samples exist and the interaction of the metal surface with oxygen can be considered as one of the most prevalent and basic reactions. Here, photoemission techniques (both X-ray and ultraviolet photoelectron spectroscopy) have been used to study the initial stages of metal oxidation of polycrystalline thorium, uranium, plutonium and sputter deposited thin films of neptunium and americium. Although the initial stages of oxidation have previously been reported for thorium, uranium[1] and plutonium[2], this represents the first investigation of neptunium and americium. The data for thorium, uranium and plutonium have been re-acquired and the full five sets of data have been subjected to identical treatment.

Finally, an update on our on going investigation into the unoccupied DOS using inverse photoemission will be presented.

.

[1] For example see W. McLean, C. A. Colmenares and R. L. Smith, Phys. Rev. B, 25 (1982) 8.
[2] D. T. Larson, J. Vac. Sci. Technol., 17 (1980) 55. T. Almeida, L. E. Cox, J. W. Ward and J, R. Naegele, Surf. Sci., 287/288 (1993) 141.

# A First-Principles Electronic Structure Study of the High-Symmetry Surfaces of FCC Americium

D. Gao and A. K. Ray

Department of Physics, the University of Texas at Arlington, Arlington, TX 76019

## INTRODUCTION

The electronic structures of the actinides are of major scientific and technological interest, partly because of the fascinating and remarkable properties of the 5*f* electrons and partly because of the enormous potentials of the actinides in nuclear applications. Similar to its nearest neighbor plutonium, americium occupies a pivotal position in actinides regarding the 5*f* electron properties.[1] In view of that, a systematic and comparative study of both plutonium and americium surface properties provides an effective way to probe the *5f* electron properties and their roles in chemical bonding. As a continuation of our research in actinide surface chemistry and physics,[2] this work has focused on the properties of fcc americium (110), (001) and (111) surfaces. In addition, the present study provides a *first* detailed comparison of the fcc americium surface properties with corresponding fcc δ-plutonium surface properties.

## COMPUTATIONAL METHOD AND RESULTS

The computational formalism used in this study is an all-electron full-potential method with a mixed basis set of linearized-augmented-plane-wave (LAPW) and augmented-plane-wave plus local orbitals (APW+lo),with and without spin-orbit coupling (SO)[3]. The generalized-gradient-approximation (GGA) to density functional theory (DFT) with a gradient corrected Perdew–Berke–Ernzerhof (PBE) functional is used. A constant muffin-tin radius ($R_{mt}$) of 2.60 a.u and large plane-wave cut-off $K_{max}$ determined by $R_{mt}K_{max}$=9.0 are used for all calculations. The surfaces of fcc americium are modeled by periodically repeated slabs of *N* americium layers (with one atom per layer and *N*=1-7) separated by a vacuum gap of 80 a.u. Twenty-one irreducible K-points have been used for reciprocal-space integrations in the surface calculations. The energy convergence criterion is set at 0.01mRy. Six theoretical levels of approximation, namely NSP-NSO, NSP-SO, SP-NSO, SP-SO, AFM-NSO, AFM-SO have been implemented in our calculations.

Detailed electronic structure calculations have been performed and will be reported for all surfaces. The ground states of all surfaces are found to be at the AFM-SO level, similar to bulk fcc Am. To obtain an idea of quantum size effects in particular, we have calculated the spin-polarization energies, spin-orbit coupling energies, work functions, and surface energies for the three americium surfaces at six different theoretical levels. The lattice constants used are the optimized lattice constants of bulk fcc Am at six different levels of theory. For the sake of brevity,

we show a comparison of *only the surface energies and the work functions for the (111) and (001) surfaces* in the figure below.

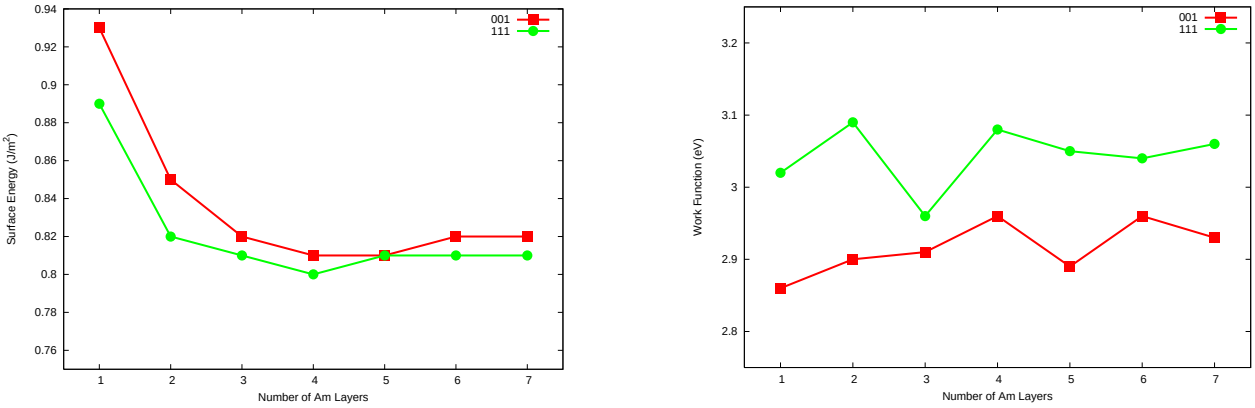


Our results show that the (111) surface has the lowest surface energy and the (110) surface has the highest surface energy. The work functions of Am surfaces have a decreasing sequence as (111) →(001)→(110). Similar trends have been observed for the δ-Pu surface. At the AFM-NSO and AFM-SO levels, the magnetic moments show a behavior of oscillation, which becomes smaller with the increase in the number of layers, and gradually the magnetic moments approach the bulk value of zero. Spin-orbit coupling can lower the total energy of, for example, fcc Am (111) films by 7.62-8.72 eV/atom, while spin-polarization decreases the total energy only by 1.50-2.79 eV/atom. The work function of fcc Am (111) surface at the ground state is predicted to be 3.06 eV. It is also found that the work function of this surface shows some oscillations when the number of layers is less than five, while it becomes relatively stable when the number of layers is greater than five, suggesting that a 5-layer film might be necessary for any future chemisorption investigation that requires an accurate prediction of the adsorbate-induced work function shift.

*This work is supported by the Chemical Sciences, Geosciences and Biosciences Division, Office of Basic Energy Sciences, Office of Science, U. S. Department of Energy (Grant No. DE-FG02-03ER15409) and the Welch Foundation, Houston, Texas (Grant No. Y-1525).*

1 S. Heathman, R. G. Haire, T. Le Bihan, A. Lindbaum, K. Litfin, Y. Méresse, and H. Libotte, Phys. Rev. Lett. **85**, 2961 (2000).

2. X. Wu and A. K. Ray, Phys. Rev. B **72**, 045115 (2005); A. K. Ray and J. C. Boettger, Phys. Rev. B **70**, 085418 (2004); J. C. Boettger and A. K. Ray, Int. J. Quant. Chem., **105**, 564 (2005); M. N. Huda and A. K. Ray, Eur. Phys. J. B **40,** 337 (2004); Physica B **352**, 5 (2004); Eur. Phys. J. B **43**, 131 (2005); Physica B **366,** 95 (2005); Phys. Rev. B **72**, 085101 (2005); Int. J. Quant. Chem. **105,** 280 (2005); H. R. Gong and A. K. Ray, Eur. Phys. J. B, **48**, 409 (2005); H. R. Gong and A. K. Ray, Proc. MRS Fall 2005 Symposium; accepted for publication; Surf. Sci. accepted for publication; D. Gao and A. K. Ray, Eur. Phys. J. B, in press; Proc. MRS Fall 2005 Symposium; accepted for publication; D. Gao and A. K. Ray, submitted for publication..

3. K. Schwarz, P. Blaha, and G. K. H. Madsen, Comp. Phys. Comm. **147,** 71 (2002).